

**RI 8875**

Bureau of Mines Report of Investigations/1984

# **Estimating Horizontal Drain Design by the Finite-Element and Finite-Difference Methods**

By D. R. Tesarik and C. D. Kealy



**UNITED STATES DEPARTMENT OF THE INTERIOR**

**Report of Investigations 8875**

# **Estimating Horizontal Drain Design by the Finite-Element and Finite-Difference Methods**

**By D. R. Tesarik and C. D. Kealy**



**UNITED STATES DEPARTMENT OF THE INTERIOR**  
**William P. Clark, Secretary**

**BUREAU OF MINES**  
**Robert C. Horton, Director**

Library of Congress Cataloging in Publication Data:

**Tesarik, D. R. (Douglas R.)**

Estimating horizontal drain design by the finite-element and finite-difference methods.

(Bureau of Mines report of investigations ; 8875)

Bibliography: p. 26.

Supt. of Docs. no.: I 28.23:8875.

1. Tailings embankments — Drainage systems — Mathematical models.  
2. Finite element method. 3. Finite differences. I. Kealy, C. D. II. Title. III.  
Series; Report of investigations (United States. Bureau of Mines) ; 8875.

TN23.U43

[TD899.M47]

622s [622'.5]

84-600030

## CONTENTS

	Page		Page
Abstract . . . . .	1	Laboratory-model tests . . . . .	6
Introduction . . . . .	2	Laboratory versus computer models . . . . .	11
Acknowledgments . . . . .	2	Comparison with other laboratory data . . . . .	14
Method . . . . .	3	Computer codes versus field data . . . . .	14
Laboratory model . . . . .	3	Dimensionless phreatic profiles . . . . .	15
Finite-difference code . . . . .	5	Conclusions and limitations . . . . .	25
Finite-element code . . . . .	6	References . . . . .	26

## ILLUSTRATIONS

1. Bureau of Mines laboratory embankment model . . . . .	3
2. Cross section of laboratory embankment model . . . . .	4
3. Plan view of laboratory model . . . . .	4
4. Grain-size curve for sand sample from laboratory model . . . . .	5
5. Moisture-density curve for sand used in laboratory model . . . . .	5
6. Boundary conditions for finite-difference model . . . . .	5
7. Cross section of three-dimensional mesh . . . . .	6
Piezometric data for laboratory embankment model:	
8. No drains, headwater height = 19.4 in . . . . .	7
9. Drains 1 and 9 inserted 2 ft, headwater height = 19.3 in . . . . .	7
10. Drains 1 and 9 inserted 4 ft, headwater height = 19.3 in . . . . .	7
11. Drains 1 and 9 inserted 6 ft, headwater height = 19.3 in . . . . .	7
12. Drains 1 and 9 inserted 6 ft, drain 5 inserted 2 ft, headwater height = 19.2 in . . . . .	7
13. Drains 1 and 9 inserted 6 ft, drain 5 inserted 4 ft, headwater height = 19.2 in . . . . .	7
14. Drains 1, 5, and 9 inserted 6 ft, headwater height = 19.3 in . . . . .	8
15. Drains 1, 5, and 9 inserted 6 ft, drains 3 and 7 inserted 2 ft, headwater height = 19.3 in . . . . .	8
16. Drains 1, 5, and 9 inserted 6 ft, drains 3 and 7 inserted 4 ft, headwater height = 19.3 in . . . . .	8
17. Drains 1, 3, 5, 7, and 9 inserted 6 ft, headwater height = 19.3 in . . . . .	8
18. Drains 1, 3, 5, 7, and 9 inserted 6 ft, drains 2, 4, 6, and 8 inserted 4 ft, headwater height = 19.5 in . . . . .	8
19. All drains inserted 6 ft, headwater height = 19.5 in . . . . .	8
20. Drains 1, 3, 5, 7, and 9 inserted 6 ft, drains 2, 4, 6, and 8 inserted 4 ft, headwater height = 21.7 in . . . . .	9
21. Drains 1, 3, 5, 7, and 9 inserted 6 ft, drains 2, 4, 6, and 8 inserted 2 ft, headwater height = 21.6 in . . . . .	9
22. Drains 1, 3, 5, 7, and 9 inserted 6 ft, headwater height = 21.7 in . . . . .	9
23. Drains 1, 5, and 9 inserted 6 ft, drains 3 and 7 inserted 4 ft, headwater height = 21.7 in . . . . .	9
24. Drains 1, 5, and 9 inserted 6 ft, drains 3 and 7 inserted 2 ft, headwater height = 21.8 in . . . . .	9
25. Drains 1, 5, and 9 inserted 6 ft, headwater height = 21.7 in . . . . .	9
26. Drains 1 and 9 inserted 6 ft, drain 5 inserted 4 ft, headwater height = 21.8 in . . . . .	10
27. Drains 1 and 9 inserted 6 ft, drain 5 inserted 2 ft, headwater height = 21.8 in . . . . .	10
28. Drains 1 and 9 inserted 6 ft, headwater height = 21.8 in . . . . .	10
29. Drains 1 and 9 inserted 4 ft, headwater height = 21.8 in . . . . .	10
30. Drains 1 and 9 inserted 2 ft, headwater height = 21.8 in . . . . .	10
31. No drains, headwater height = 21.2 in . . . . .	10
32. Phreatic surface, laboratory model versus finite-difference method; no drains . . . . .	11
Phreatic surface between drains, laboratory model versus finite-difference method:	
33. 24-in drains, 36-in spacing . . . . .	11
34. 24-in drains, 72-in spacing . . . . .	12
35. 48-in drains, 72-in spacing . . . . .	12
36. 72-in drains, 18-in spacing . . . . .	12
37. 72-in drains, 36-in spacing . . . . .	13
38. 72-in drains, 72-in spacing . . . . .	13
39. Phreatic surface between drains, finite-element method versus finite-difference method . . . . .	13
Three-dimensional finite-element results versus piezometric elevations from Kenney, Pazin, and Choi (7):	
40. 27-in drains, 32-in spacing . . . . .	14
41. No drains . . . . .	14

## ILLUSTRATIONS—Continued

	Page
42. Section of drain arrays showing area modeled using finite-difference code . . . . .	15
43. Section E-E' from figure 42, Sohio Western Mining Co. tailings embankment . . . . .	15
44. Cross section between filter pads, Union Carbide Corp. tailings embankment . . . . .	15
 Dimensionless phreatic profiles:	
45. $H/L = 0.2$ , $1/L = 0.25$ . . . . .	16
46. $H/L = 0.25$ , $1/L = 0.25$ . . . . .	16
47. $H/L = 0.3$ , $1/L = 0.25$ . . . . .	17
48. $H/L = 0.35$ , $1/L = 0.25$ . . . . .	17
49. $H/L = 0.4$ , $1/L = 0.25$ . . . . .	17
50. $H/L = 0.45$ , $1/L = 0.25$ . . . . .	18
51. $H/L = 0.5$ , $1/L = 0.25$ . . . . .	18
52. $H/L = 0.2$ , $1/L = 0.375$ . . . . .	19
53. $H/L = 0.25$ , $1/L = 0.375$ . . . . .	19
54. $H/L = 0.3$ , $1/L = 0.375$ . . . . .	19
55. $H/L = 0.35$ , $1/L = 0.375$ . . . . .	20
56. $H/L = 0.4$ , $1/L = 0.375$ . . . . .	20
57. $H/L = 0.45$ , $1/L = 0.375$ . . . . .	21
58. $H/L = 0.5$ , $1/L = 0.375$ . . . . .	21
59. $H/L = 0.2$ , $1/L = 0.5$ . . . . .	22
60. $H/L = 0.25$ , $1/L = 0.5$ . . . . .	22
61. $H/L = 0.3$ , $1/L = 0.5$ . . . . .	22
62. $H/L = 0.35$ , $1/L = 0.5$ . . . . .	23
63. $H/L = 0.4$ , $1/L = 0.5$ . . . . .	23
64. $H/L = 0.45$ , $1/L = 0.5$ . . . . .	24
65. $H/L = 0.5$ , $1/L = 0.5$ . . . . .	24
66. Embankment cross section plotted using dimensionless graphs . . . . .	25
67. Slip circles for embankment plotted in figure 66 . . . . .	25

## TABLES

1. Conversion from dimensionless graph values to units used in example, drains 50 ft apart . . . . .	25
2. Conversion from dimensionless graph values to units used in example, no-drains case . . . . .	25

### UNIT OF MEASURE ABBREVIATIONS USED IN THIS REPORT

cm/s	centimeter per second	mm	millimeter
ft	foot	pct	percent
ga	gauge	pcf	pound per cubic foot
lb/ft <sup>3</sup>	pound per cubic foot	psi	pound per square inch
pct	percent	yr	year

# ESTIMATING HORIZONTAL DRAIN DESIGN BY THE FINITE-ELEMENT AND FINITE-DIFFERENCE METHODS

By D. R. Tesarik<sup>1</sup> and C. D. Kealy<sup>2</sup>

---

## ABSTRACT

To ensure the stability of a tailings pond embankment, the height of the phreatic surface must be kept at or below a safe level. In this investigation, the Bureau of Mines analyzed various horizontal drain designs for tailings embankments to determine their effects on location of the phreatic surface. This report describes the investigation, and it includes 21 dimensionless graphs that can be used to estimate the drain spacing and length dimensions necessary to ensure the stability of embankments of various configurations.

Analyses were based on the use of two computer codes, a three-dimensional finite-element code and a two-dimensional finite-difference code. The computer-generated results were compared with results obtained from a laboratory embankment model, other laboratory test results, and piezometric data from two actual tailings embankments.

Nearly the same phreatic surface locations were predicted using either of the computer codes. For one of the actual embankments studied, the predicted phreatic surface location was slightly higher than the measured location; for the other, the predicted location closely followed the actual surface trend. Phreatic surfaces of the laboratory model were slightly higher than the code-generated locations, and the differences grew larger as drain length increased or drain spacing decreased.

---

<sup>1</sup>Mathematician.

<sup>2</sup>Supervisory mining engineer.

Spokane Research Center, Bureau of Mines, Spokane, WA.

## INTRODUCTION

The presence of ground water is one of the most critical factors contributing to the instability of tailings embankments. The height of the phreatic surface has been shown to play a critical role in determining the factor of safety, the traditional measure of stability for earth embankments (10).<sup>3</sup> Nonexistent or inefficient drainage facilities usually result in a high phreatic surface that can ultimately cause the embankment to fail. If the height of the phreatic surface can be reduced, the factor of safety will increase dramatically. One possible solution, especially for remedial situations, is the installation of horizontal drains. In planning a horizontal drain system, the design engineer is faced with the problem of determining what drain dimensions (spacing and length) are necessary to reduce the phreatic surface enough to ensure an acceptable factor of safety. Various analytical techniques are available for solving this problem.

The use of two-dimensional techniques to determine seepage characteristics in embankments without drains has become a common engineering practice (3-6, 11-14). The effects of toe drains or blanket drains can also be modeled

with two-dimensional codes, provided all cross sections of the embankment are the same. The design of horizontal drains, however, is a three-dimensional problem, and analysis can be time consuming. Three-dimensional finite-element meshes require considerable time to construct, and three-dimensional finite-element codes often require much computer time and space due to the large number of unknown values that must be computed.

This Bureau of Mines report presents guidelines in a graphic format for field installation of horizontal drains. For various combinations of drain lengths and spacings, each of the dimensionless graphs show the cross section of an embankment between horizontal drains. They enable the user to estimate the location of the phreatic surface. Using these graphs, a mine operator can evaluate the feasibility of a proposed drain design. Thorough site investigations may reveal lenses, perched water tables, or other embankment anomalies that could alter the initial estimation for drain placement (1), and a detailed three-dimensional finite-element analysis may be desirable.

## ACKNOWLEDGMENTS

The authors wish to thank Fred Tracy, supervisory computer scientist, U.S. Army Engineer Division, U.S. Army Engineer Waterways Experiment Station, Vicksburg, MS, for assistance in using the three-dimensional finite-element

computer program; and John P. Sanders, plant superintendent, Union Carbide Corp., Metals Div., Hot Springs, AR, for providing piezometric data and data on embankment geometry.

<sup>3</sup>Underlined numbers in parentheses refer to items in the list of references at the end of this report.

## METHOD

The graphs showing predicted phreatic surface levels between horizontal drains (presented in the "Dimensionless Phreatic Profiles" section) are results of a two-dimensional finite-difference analysis. These data were compared to a laboratory model, a three-dimensional finite-element analysis (12), other laboratory tests (7), and two actual field situations. Since the predicted phreatic surfaces between the drains correlated well with results obtained using these other

data and methods, the graphs were constructed using the finite-difference method.

The above analysis indicated that the phreatic surface arches between drains, with the highest elevation at mid-point. Since the factor of safety of an embankment calculated using two-dimensional methods will be at its lower bound at this point, the dimensionless graphs represent a conservative condition in this respect.

## LABORATORY MODEL

A 96- by 72-in model tank was constructed of 12-ga cold-rolled steel with welded seams and mounted on a structural steel framework on dollies (fig. 1). The inside walls and floor were coated with latex-base paint. While still wet, the surfaces were sprinkled with 16-mesh sand to prevent flow channels from developing along the sides and bottom of the tank.

Clusters of piezometers of increasing height were installed as shown in figures 2 and 3. They were constructed of 5/32-in-ID copper tubing with 150-mesh screen soldered to the top of each tube. The screen was covered with filter cloth. Plexiglas<sup>4</sup> plastic viewing tubes connected to the piezometers were mounted to the side of the model. A blue dye was injected into each tube for ease of reading.

<sup>4</sup>Reference to specific products does not imply endorsement by the Bureau of Mines.

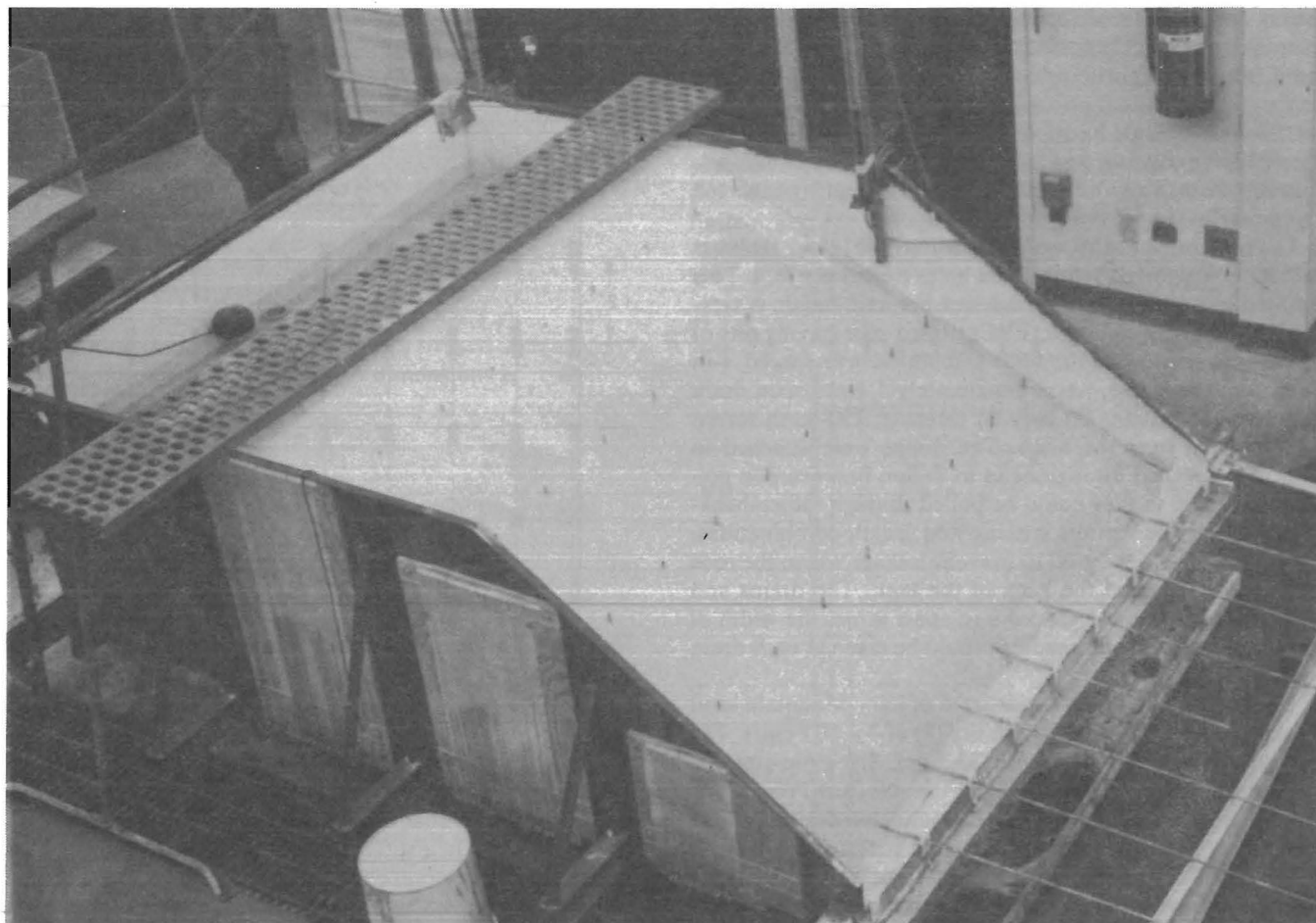


FIGURE 1. — Bureau of Mines laboratory embankment model.

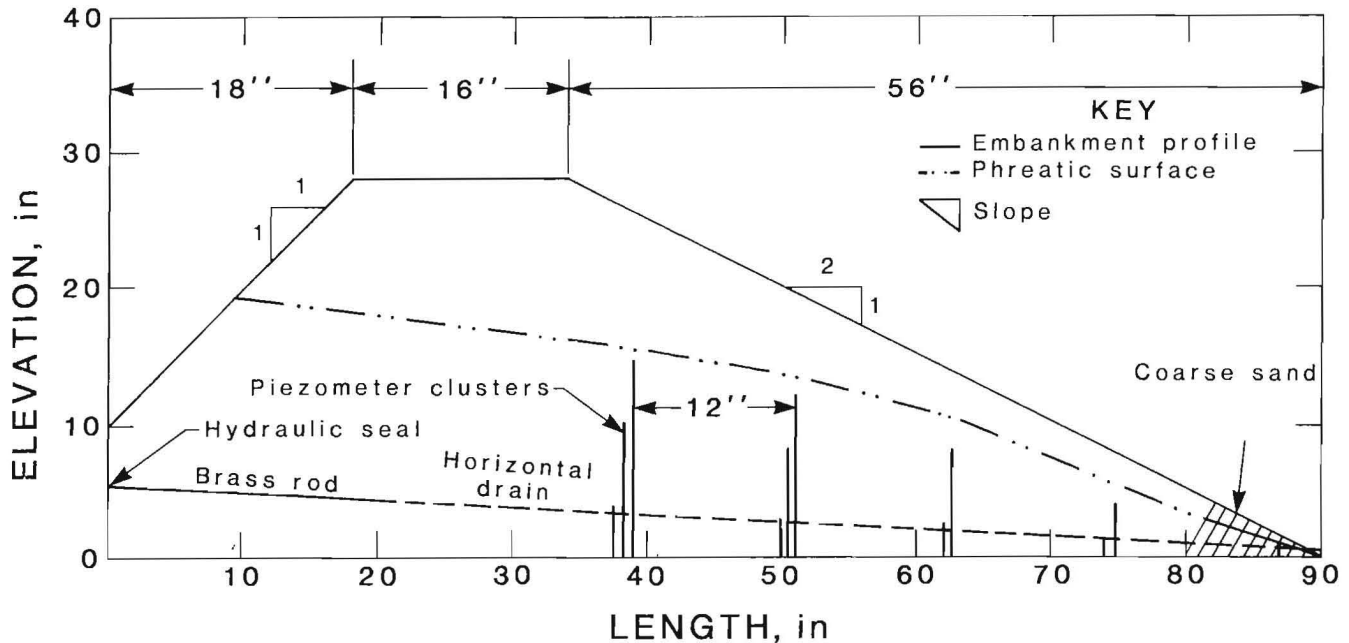


FIGURE 2. — Cross section of laboratory embankment model.

Some of the filters on the piezometers became clogged during initial tests, so open-well piezometers were subsequently installed. They were constructed of 1/4-in-ID perforated brass tubing with 140-mesh screen soldered over the perforations and bottom end of each tube. The tubes were installed at the same locations as the piezometer clusters (fig. 3), excluding the first row near the toe of the embankment. Piezometer readings were taken with a voltmeter connected to an insulated wire with exposed ends.

The horizontal drains were constructed of 1/4-in-ID brass tubing with eighteen 1/8-in-diam holes drilled per foot. This resulted in a 2.3-pct open drain area per unit length. A typical 2-in polyvinyl chloride (PVC) slotted pipe having sets of three 1/64-in slots around the circumference, spaced 1-in apart along the pipe, has approximately 1.4 pct open drain area per unit length. To prevent clogging, 150-mesh screen was soldered over the holes. The drains were attached to rods and threaded through holes in Teflon fluorocarbon polymer brackets so they could be pulled through the embankment to achieve various spacing and length combinations. Hydraulic seals were used to prevent leakage where the rods were pulled through the back of the tank. The drains and piezometer tubes were spaced 9 in apart across the width of the tank so piezometer readings could be taken at each drain location.

The embankment was constructed of Lane Mountain sand (Valley, WA) having a permeability ( $k$ ) of  $3 \times 10^{-4}$  cm/s. The dry density of the material was 83.3 pcf. The grain-size distribution is shown in figure 4, and the standard Proctor test results are shown in figure 5. Consolidated-drained direct shear tests yielded an angle of internal friction of  $37^\circ$  and a cohesion of 9 psi. The downstream slope was 2:1 and the upstream slope was 1:1 (fig. 2). The embankment was compacted by hand with a 3/4-in-diam pipe attached to a 1-in-thick 6-in-diam steel plate.

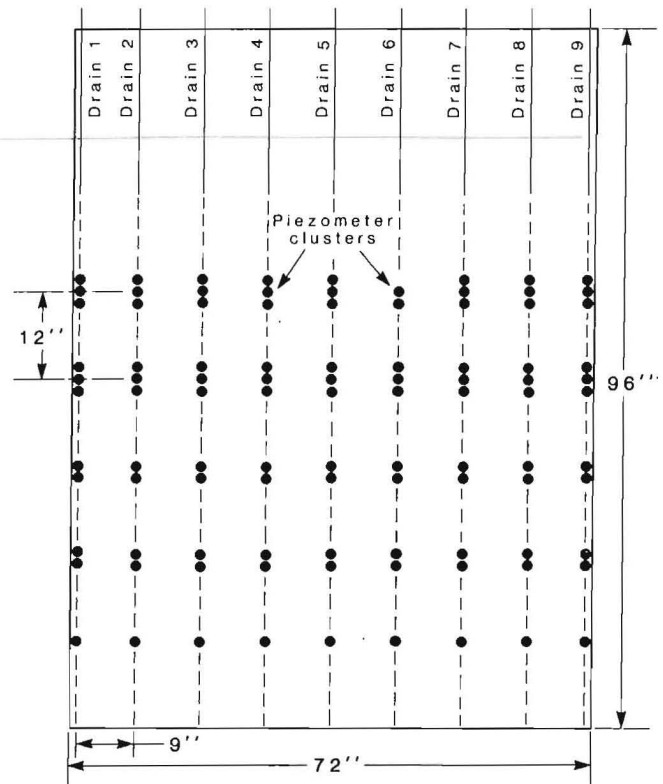


FIGURE 3. — Plan view of laboratory model.

The first trial embankment experienced progressive failure due to erosion when subjected to a headwater height of 19.3 in, so a 10-in tow drain composed of coarse sand ( $k = 3.75 \times 10^{-2}$  cm/s) was installed to increase stability. All subsequent tests were run with the toe drain. A constant upstream head was maintained during the tests by a float valve.

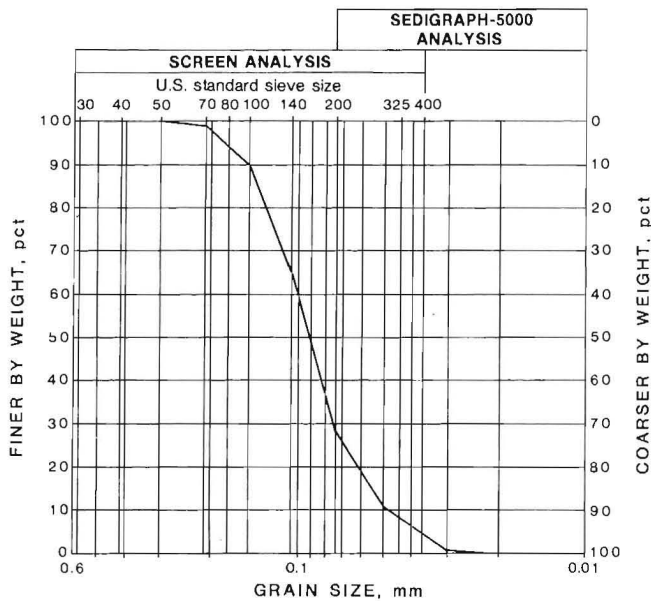


FIGURE 4. — Grain-size curve for sand sample from laboratory model.

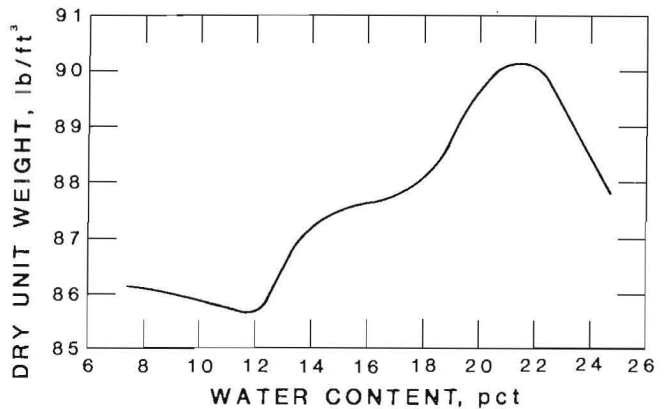


FIGURE 5. — Moisture-density curve for sand used in laboratory model.

## FINITE-DIFFERENCE CODE

The governing equations by the finite-difference computer program (14) are based on Darcy's law in two dimensions:

$$q_x = -k \frac{\partial h}{\partial x}, \quad (1)$$

$$q_y = -k \frac{\partial h}{\partial y}, \quad (2)$$

where  $q_x$  = Darcy velocity in  $x$  direction,  
 $q_y$  = Darcy velocity in  $y$  direction,  
 $k$  = permeability of the soil,  $k = k(x,y)$ ,  
 and  $h$  = total head.

The continuity equation in two dimensions is

$$\frac{\partial q_x}{\partial x} + \frac{\partial q_y}{\partial y} = 0, \quad (3)$$

Substituting equations 1 and 2 into equation 3 yields

$$\frac{\partial}{\partial x} \left( -k \frac{\partial h}{\partial x} \right) + \frac{\partial}{\partial y} \left( -k \frac{\partial h}{\partial y} \right) = 0. \quad (4)$$

If the soil (or tailings material) is assumed to be homogeneous and isotropic,<sup>5</sup> then  $k$  is independent of  $x$  and  $y$ , and equation 4 becomes Laplace's equation,

$$\frac{\partial^2 h}{\partial x^2} + \frac{\partial^2 h}{\partial y^2} = 0. \quad (5)$$

The flow region was modeled using the plan view (fig. 3). The boundary conditions are specified in figure 6.

The model did not include the  $z$  component of velocity. This condition is the Dupuit assumption, the validity of which has been evaluated analytically by Murray and Monkmeyer (9). In general, best results using the Dupuit assumption are achieved for situations where the slope of the phreatic surface is relatively flat (10:1). It will be shown later that phreatic surfaces between drains calculated with the finite-difference code and with a three-dimensional analysis compare favorably.

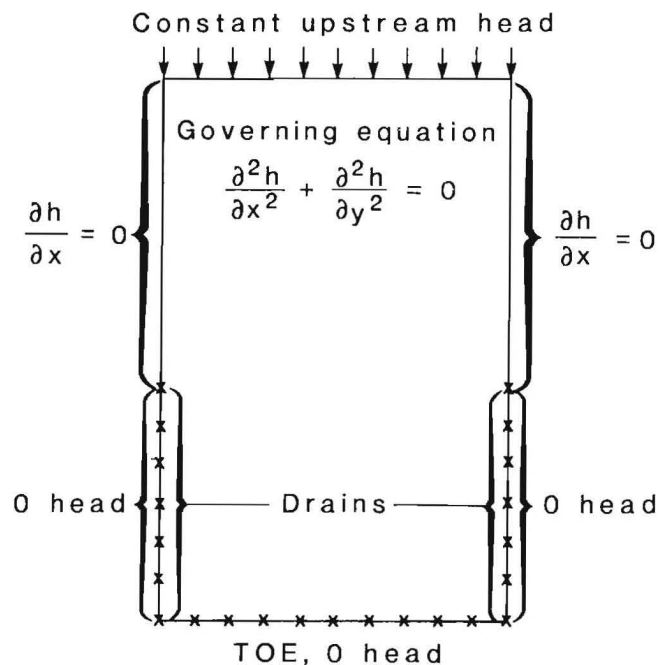


FIGURE 6. — Boundary conditions for finite-difference model.

<sup>5</sup>Horizontal permeability is often greater than vertical permeability in hydraulically placed tailings material (6). If this condition exists, it is likely that the phreatic surface will be higher than it would be in an embankment with isotropic properties.

## FINITE-ELEMENT CODE

The three-dimensional finite-element program was developed by the U.S. Army Engineer Waterways Experiment Station (12). The basic assumptions of the model are as follows:

1. The density of the soil-water complex remains constant, since its compressibility is zero.
2. The flow is laminar; hence, Darcy's law holds.

The governing equation is similar to equation 4, only it has a  $z$  component:

$$\frac{\partial}{\partial x} \left( -k \frac{\partial h}{\partial x} \right) + \frac{\partial}{\partial y} \left( -k \frac{\partial h}{\partial y} \right) + \frac{\partial}{\partial z} \left( -k \frac{\partial h}{\partial z} \right) = 0. \quad (6)$$

Since homogeneous soil conditions were assumed from this study,  $k$  is constant, and equation 6 reduces to Laplace's equation in three dimensions:

$$\frac{\partial^2 h}{\partial x^2} + \frac{\partial^2 h}{\partial y^2} + \frac{\partial^2 h}{\partial z^2} = 0. \quad (7)$$

A solution to equation 7 by the finite-element method has been discussed by Tracy (12).

A cross section of the finite-element mesh used to analyze the laboratory model is shown in figure 7. A total of 448 elements and 648 nodes were used in the simulation. The headwater entered the embankment at nodes 6, 7, and 8 and corresponding nodes in other cross sections in the  $y$  direction.

Two methods were used to simulate the drains, and each gave the same results. In the first method, elements such as 15, 22, 29, 36, 43, and 50 were assigned a  $y$  and  $z$  dimension of 0.5 and a permeability to represent the drain. The second method used zero pressure as a boundary condition at nodes such as 17, 25, 33, 41, 49, 57, and 65. The boundary conditions for both methods were applied at  $y = 0$  and  $y = \text{width}$  of the embankment so that the phreatic surface was symmetric about a line parallel to and between the drains. Various drain spacings were achieved by changing the width ( $y$  dimension) of all the elements. Drain length was changed by altering the element permeability, when the first method was used, or eliminating the boundary condition of zero pressure at a node when the second method was used.

## LABORATORY-MODEL TESTS

The drains were inserted into the embankment in the following sequence to the depths shown:

1. No drains inserted.
2. Drains 1 and 9, 2 ft.
3. Drains 1 and 9, 4 ft.
4. Drains 1 and 9, 6 ft.
5. Drains 1 and 9, 6 ft; drain 5, 2 ft.
6. Drains 1 and 9, 6 ft; drain 5, 4 ft.
7. Drains 1, 5, and 9, 6 ft.
8. Drains 1, 5, and 9, 6 ft; drains 3 and 7, 2 ft.
9. Drains 1, 5, and 9, 6 ft; drains 3 and 7, 4 ft.
10. Drains 1, 3, 5, 7, and 9, 6 ft.
11. Drains 1, 3, 5, 7, and 9, 6 ft; drains 2, 4, 6, and 8, 4 ft.
12. All drains inserted, 6 ft.

Open-well piezometer readings were taken for each drain configuration at 1-day intervals. The next drain configuration was not set up until each piezometer had the same reading for two consecutive days. The piezometric data were

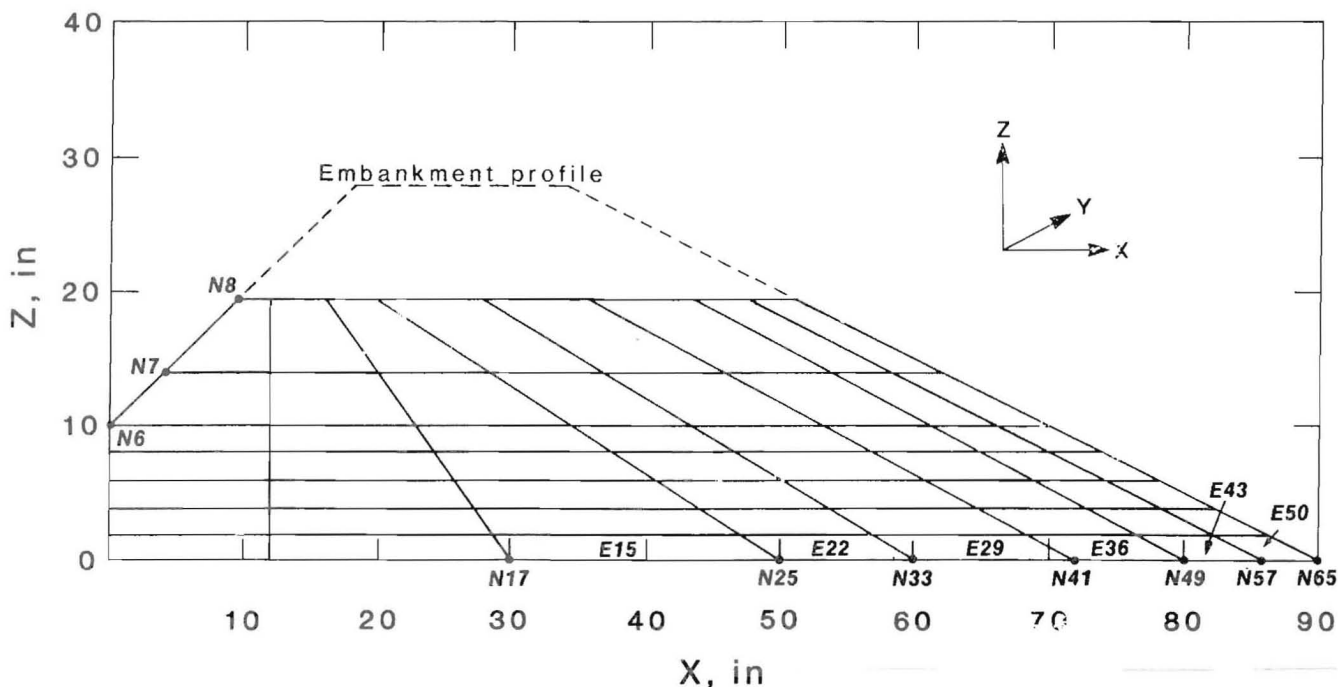


FIGURE 7. — Cross section of three-dimensional mesh. (E prefix denotes element; N denotes node.)

plotted on three-dimensional graphs for visual interpretation of the effects of the drains (figs. 8-31).

When all drains were inserted 6 ft and the phreatic surface had reached steady state, the sequence was executed in reverse order to test the integrity of the model. A one-to-one

numerical comparison of results for the two sequences is not valid, because the headwater height was increased for the second sequence. However, the piezometer responses and geometric characteristics were compatible.

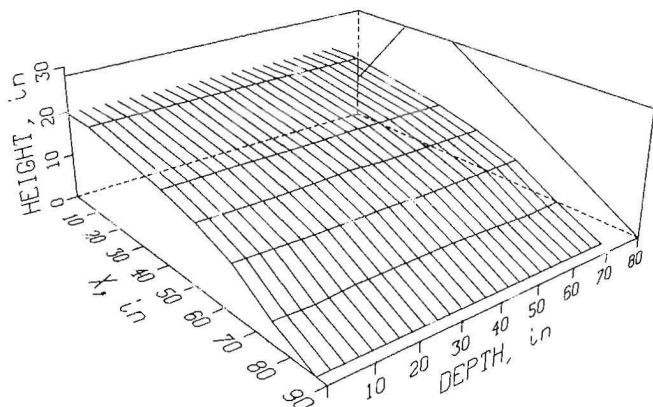


FIGURE 8. — Piezometric data for laboratory embankment model; no drains, headwater height = 19.4 in.

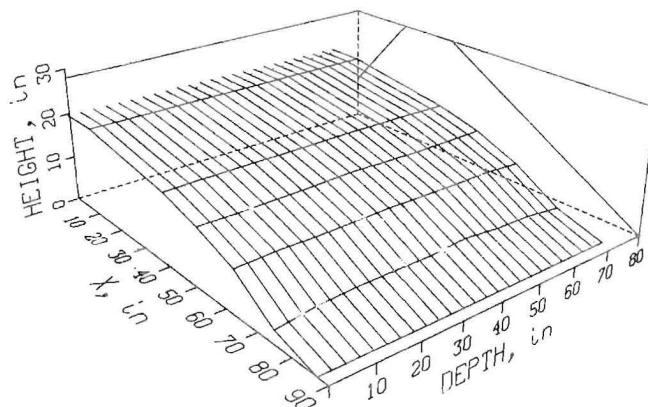


FIGURE 9. — Piezometric data for laboratory embankment model; drains 1 and 9 inserted 2 ft, headwater height = 19.3 in. (Drains are identified by number in figure 3.)

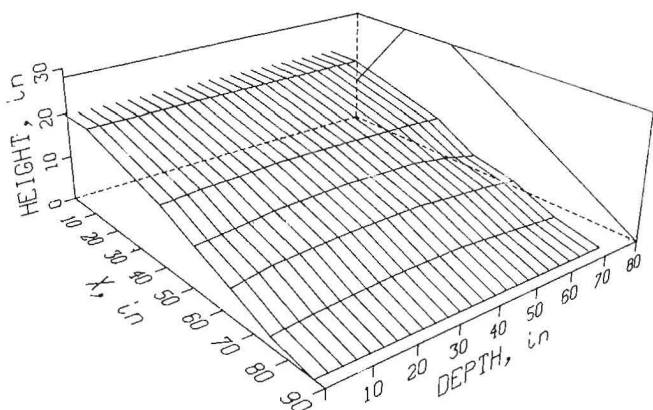


FIGURE 10. — Piezometric data for laboratory embankment model; drains 1 and 9 inserted 4 ft, headwater height = 19.3 in.

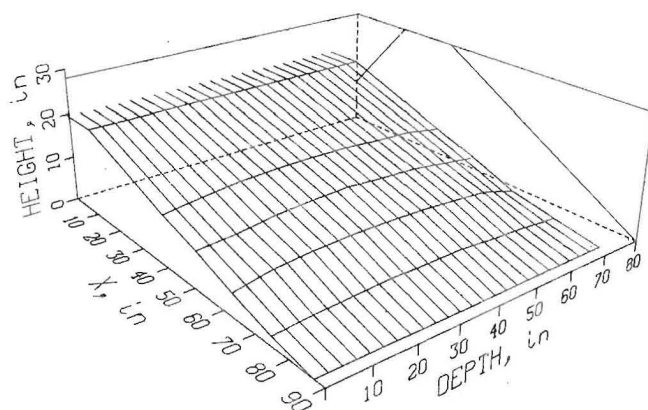


FIGURE 11. — Piezometric data for laboratory embankment model; drains 1 and 9 inserted 6 ft, headwater height = 19.3 in.

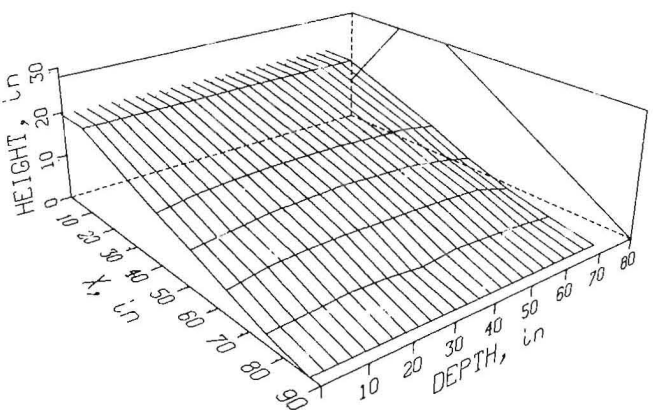


FIGURE 12. — Piezometric data for laboratory embankment model; drains 1 and 9 inserted 6 ft, drain 5 inserted 2 ft, headwater height = 19.2 in.

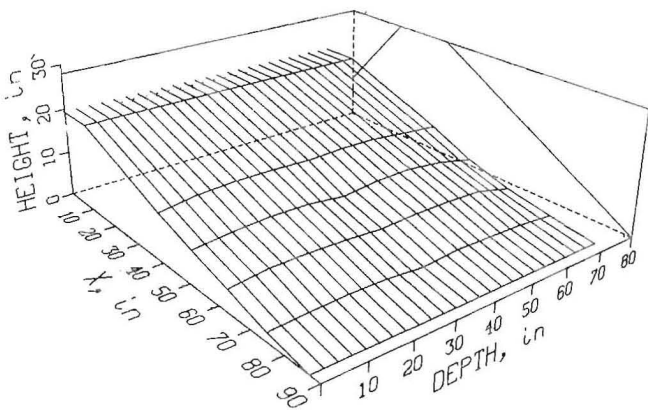


FIGURE 13. — Piezometric data for laboratory embankment model; drains 1 and 9 inserted 6 ft, drain 5 inserted 4 ft, headwater height = 19.2 in.

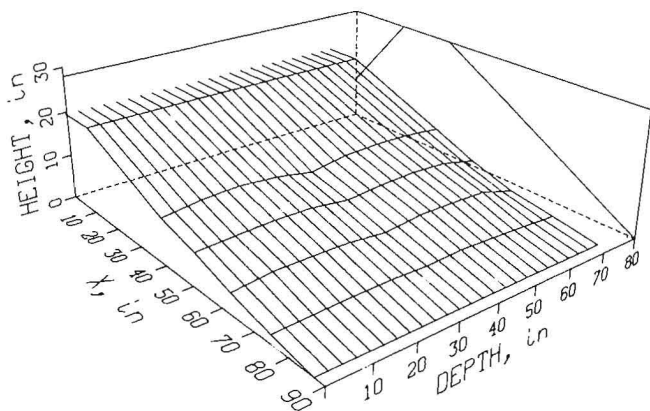


FIGURE 14. — Piezometric data for laboratory embankment model; drains 1, 5, and 9 inserted 6 ft, headwater height = 19.3 in.

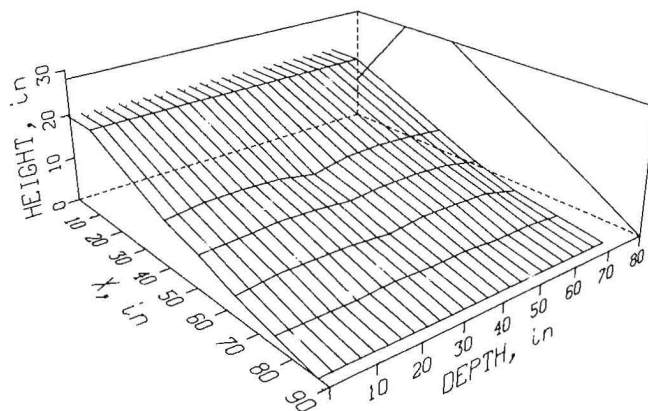


FIGURE 15. — Piezometric data for laboratory embankment model; drains 1, 5, and 9 inserted 6 ft, drains 3 and 7 inserted 2 ft, headwater height = 19.3 in.

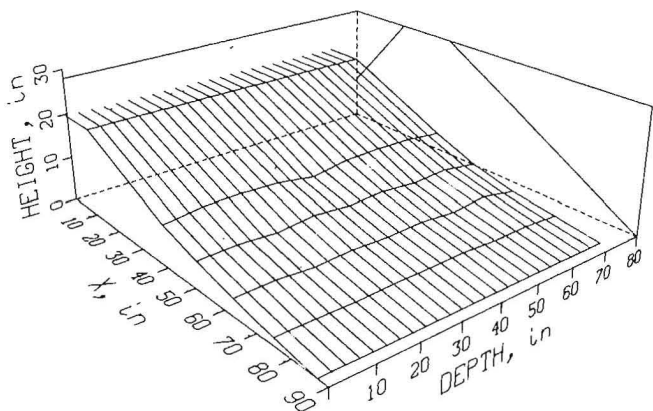


FIGURE 16. — Piezometric data for laboratory embankment model; drains 1, 5, and 9 inserted 6 ft, drains 3 and 7 inserted 4 ft, headwater height = 19.3 in.

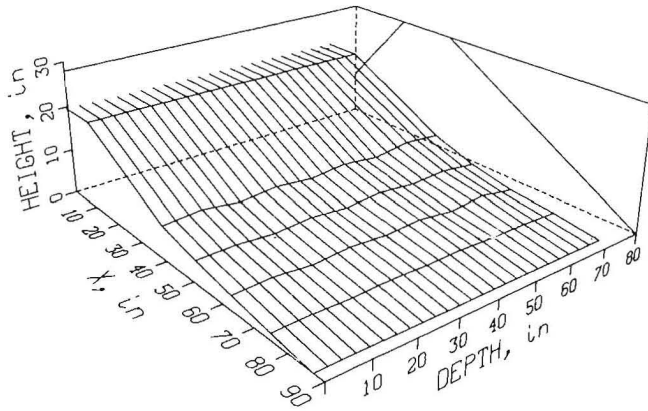


FIGURE 17. — Piezometric data for laboratory embankment model; drains 1, 3, 5, 7, and 9 inserted 6 ft, headwater height = 19.3 in.

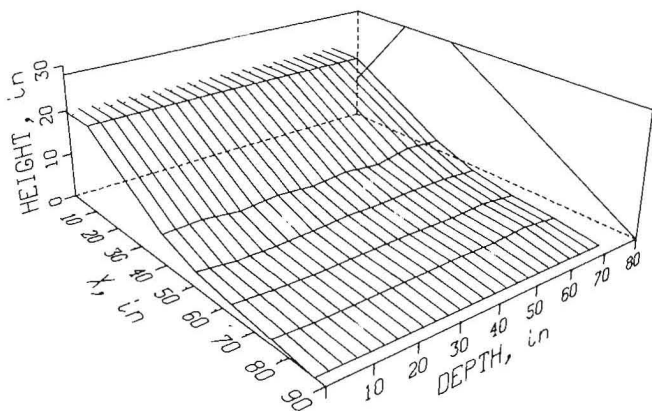


FIGURE 18. — Piezometric data for laboratory embankment model; drains 1, 3, 5, 7, and 9 inserted 6 ft, drains 2, 4, 6, and 8 inserted 4 ft, headwater height = 19.5 in.

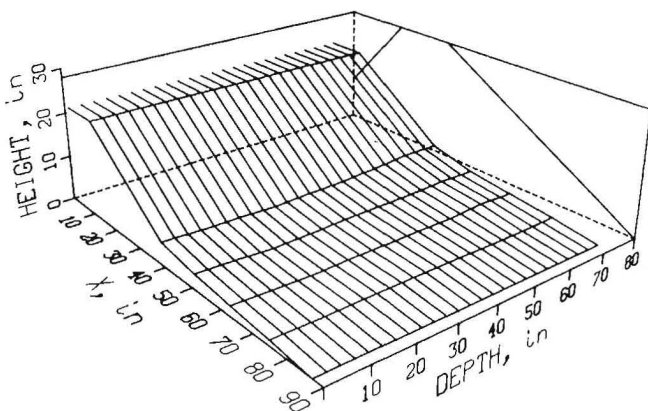


FIGURE 19. — Piezometric data for laboratory embankment model; all drains inserted 6 ft, headwater height = 19.5 in.

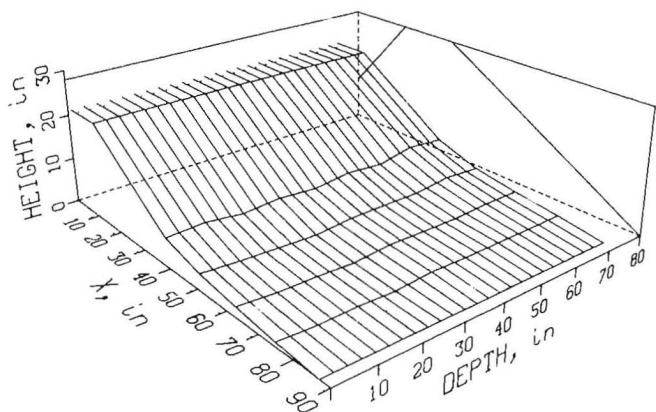


FIGURE 20. — Piezometric data for laboratory embankment model; drains 1, 3, 5, 7, and 9 inserted 6 ft, drains 2, 4, 6, and 8 inserted 4 ft, headwater height = 21.7 in.

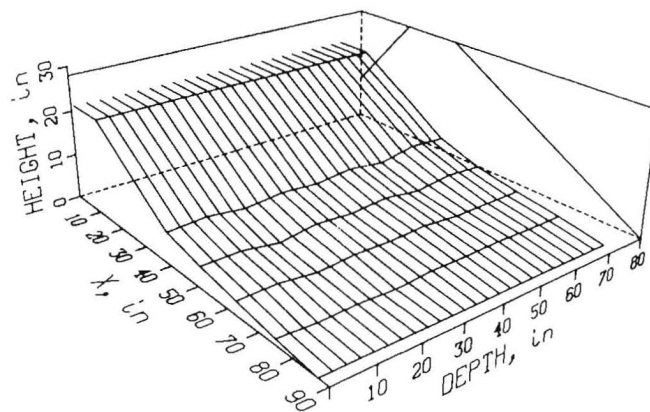


FIGURE 21. — Piezometric data for laboratory embankment model; drains 1, 3, 5, 7, and 9 inserted 6 ft, drains 2, 4, 6, and 8 inserted 2 ft, headwater height = 21.6 in.

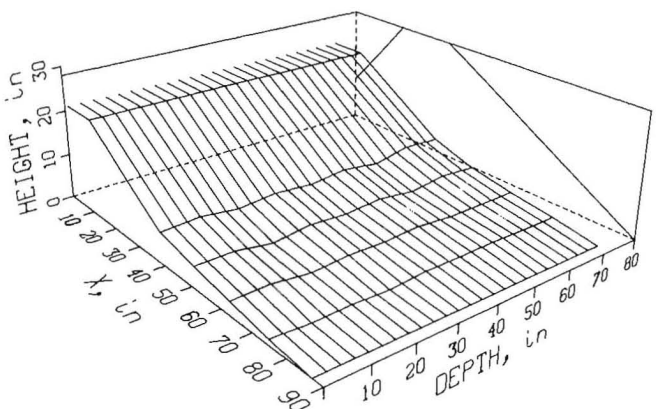


FIGURE 22. — Piezometric data for laboratory embankment model; drains 1, 3, 5, 7, and 9 inserted 6 ft, headwater height = 21.7 in.

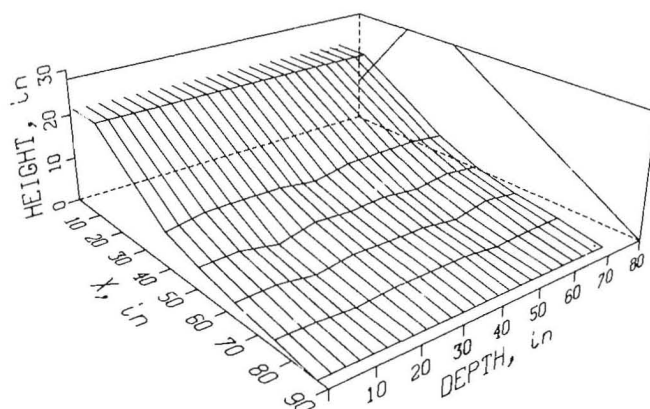


FIGURE 23. — Piezometric data for laboratory embankment model; drains 1, 5, and 9 inserted 6 ft, drains 3 and 7 inserted 4 ft, headwater height = 21.7 in.

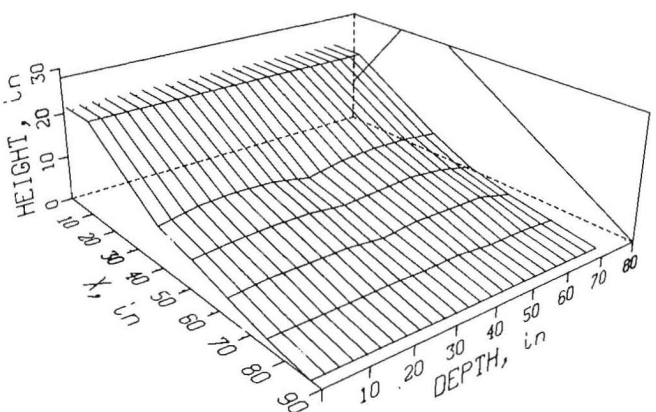


FIGURE 24. — Piezometric data for laboratory embankment model; drains 1, 5, and 9 inserted 6 ft, drains 3 and 7 inserted 2 ft, headwater height = 21.8 in.

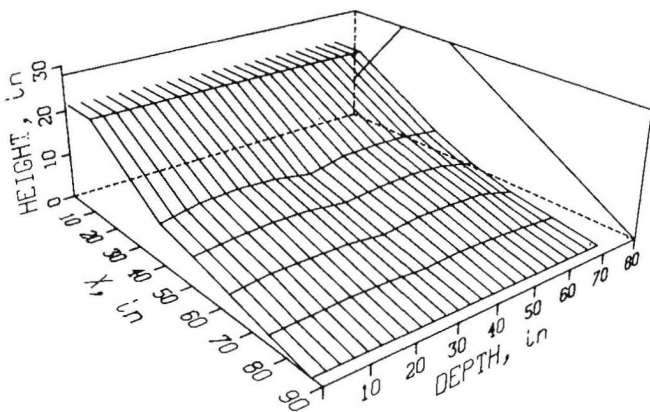


FIGURE 25. — Piezometric data for laboratory embankment model; drains 1, 5, and 9 inserted 6 ft, headwater height = 21.7 in.

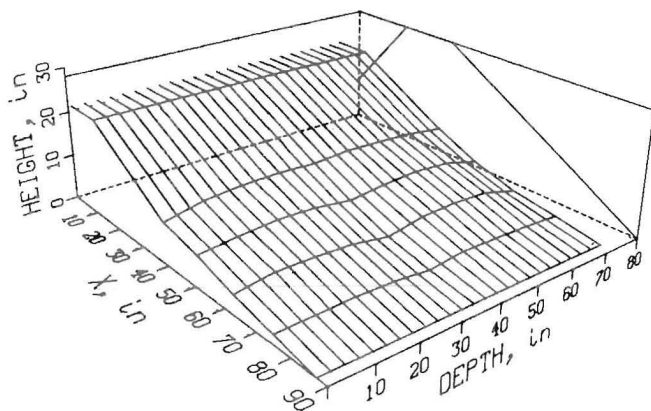


FIGURE 26. — Piezometric data for laboratory embankment model; drains 1 and 9 inserted 6 ft, drain 5 inserted 4 ft, headwater height = 21.8 in.

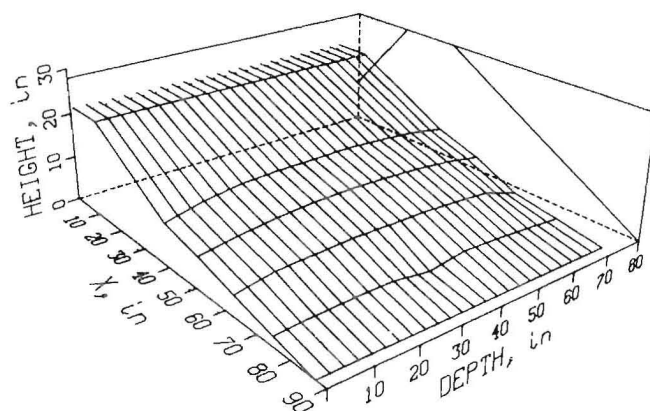


FIGURE 27. — Piezometric data for laboratory embankment model; drains 1 and 9 inserted 6 ft, drain 5 inserted 2 ft, headwater height = 21.8 in.

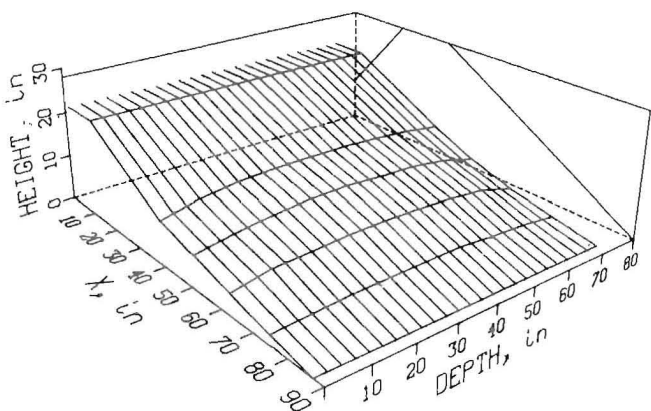


FIGURE 28. — Piezometric data for laboratory embankment model; drains 1 and 9 inserted 6 ft, headwater height = 21.8 in.

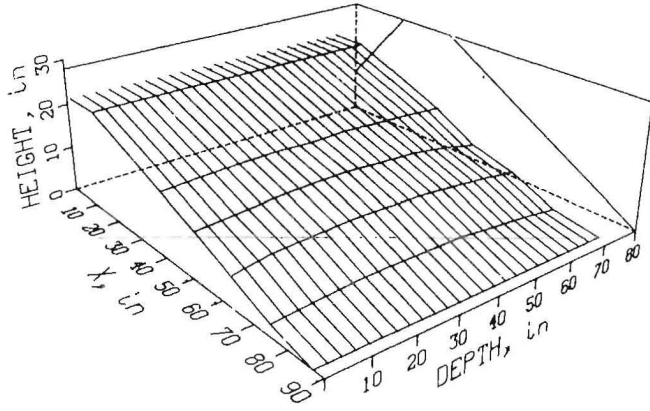


FIGURE 29. — Piezometric data for laboratory embankment model; drains 1 and 9 inserted 4 ft, headwater height = 21.8 in.

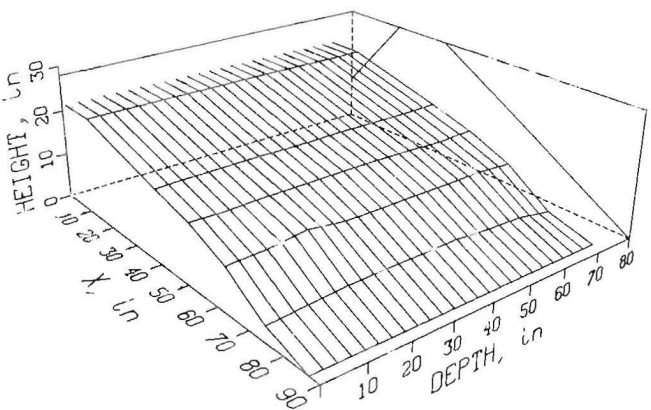


FIGURE 30. — Piezometric data for laboratory embankment model; drains 1 and 9 inserted 2 ft, headwater height = 21.8 in.

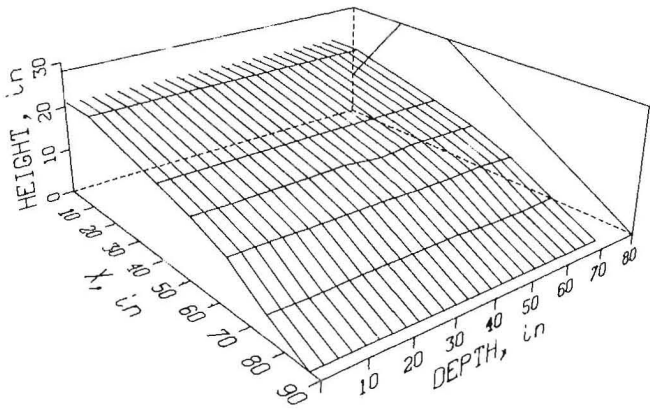


FIGURE 31. — Piezometric data for laboratory embankment model; no drains, headwater height = 21.2 in.

## LABORATORY VERSUS COMPUTER MODELS

Only the readings from the open-well piezometers were used to compare the laboratory-model results to the results from the computer codes. Although some of the piezometers in the clusters became plugged with fines, enough data were available to describe the bending of the equipotential lines near the toe of the embankment.

Profiles of the embankment at midpoint, comparing phreatic surface from the test model to those calculated using the finite-difference code, are shown in figures 32-38. These

figures show that as the drain length increased or the drain spacing decreased, the phreatic surfaces calculated from the finite-difference code started to fall below those determined using the laboratory model.

Figure 39 compares the phreatic surface between drains computed by the two computer codes for a 6-ft drain and spacings of 16, 36, and 72 in. The results indicate that the finite-difference and finite-element codes calculate nearly the same phreatic surface between drains.

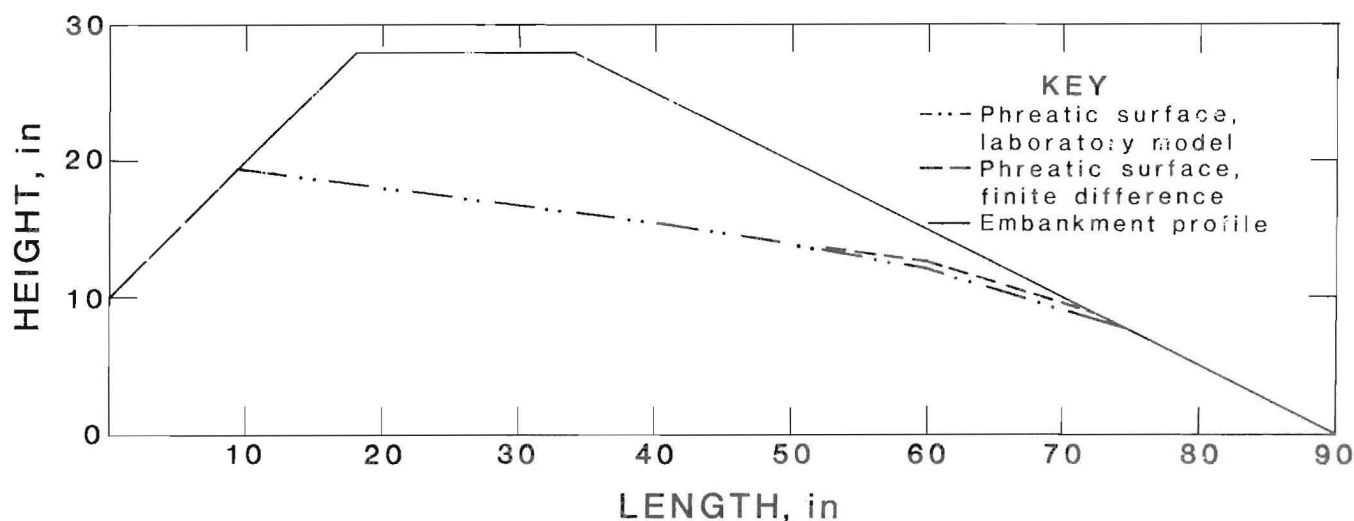


FIGURE 32. — Phreatic surface, laboratory model versus finite-difference method; no drains.

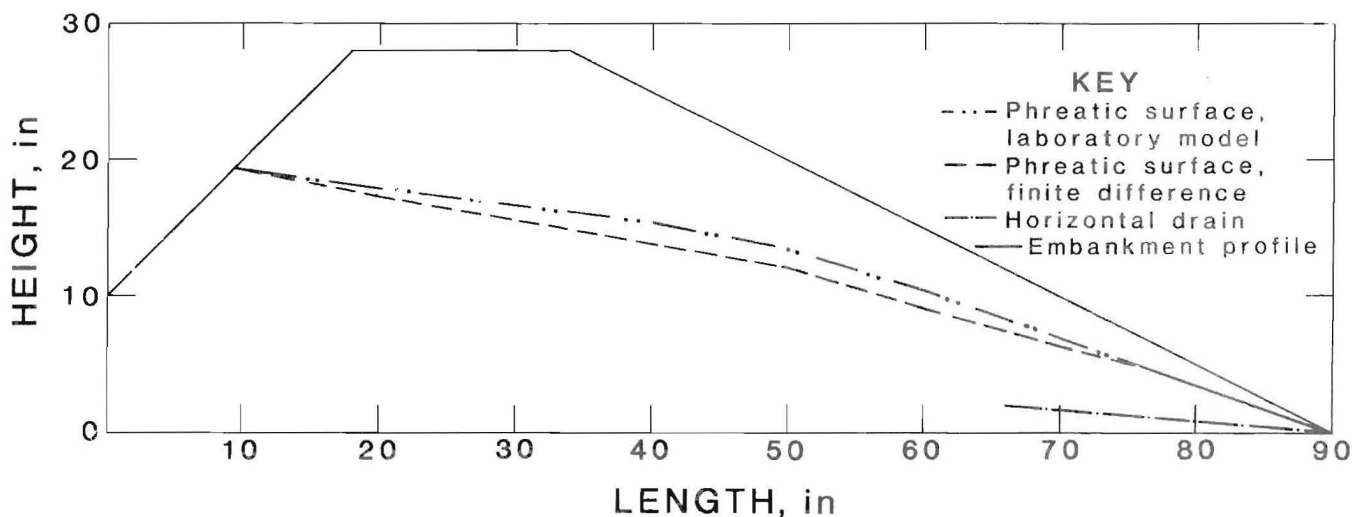


FIGURE 33. — Phreatic surface between drains, laboratory model versus finite-difference method; 24-in drains, 36-in spacing.

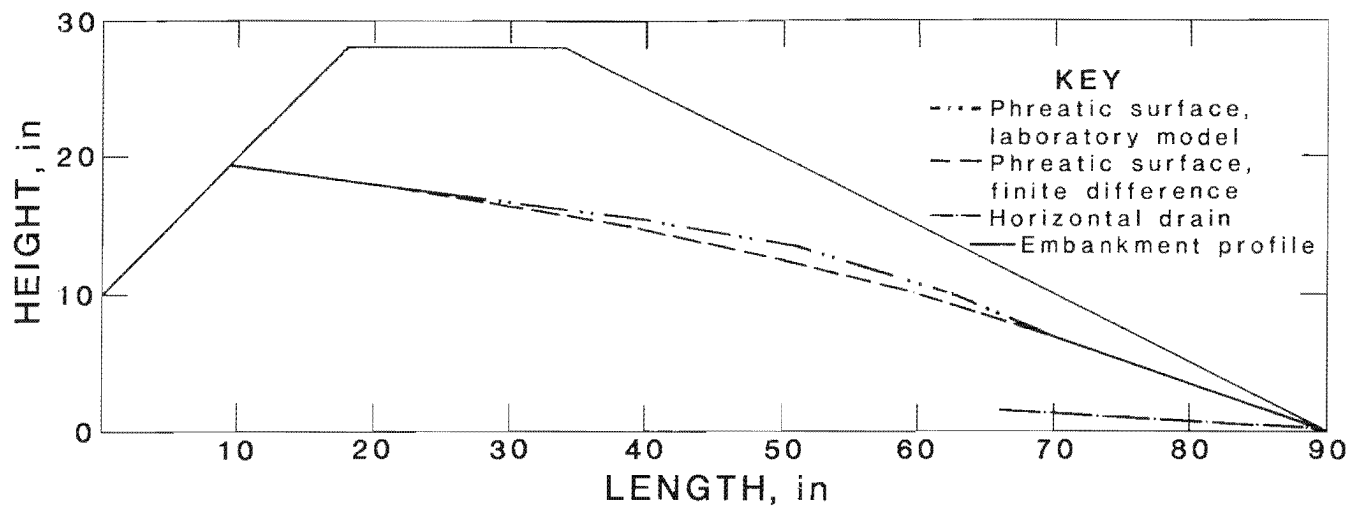


FIGURE 34. — Phreatic surface between drains, laboratory model versus finite-difference method; 24-in drains, 72-in spacing.

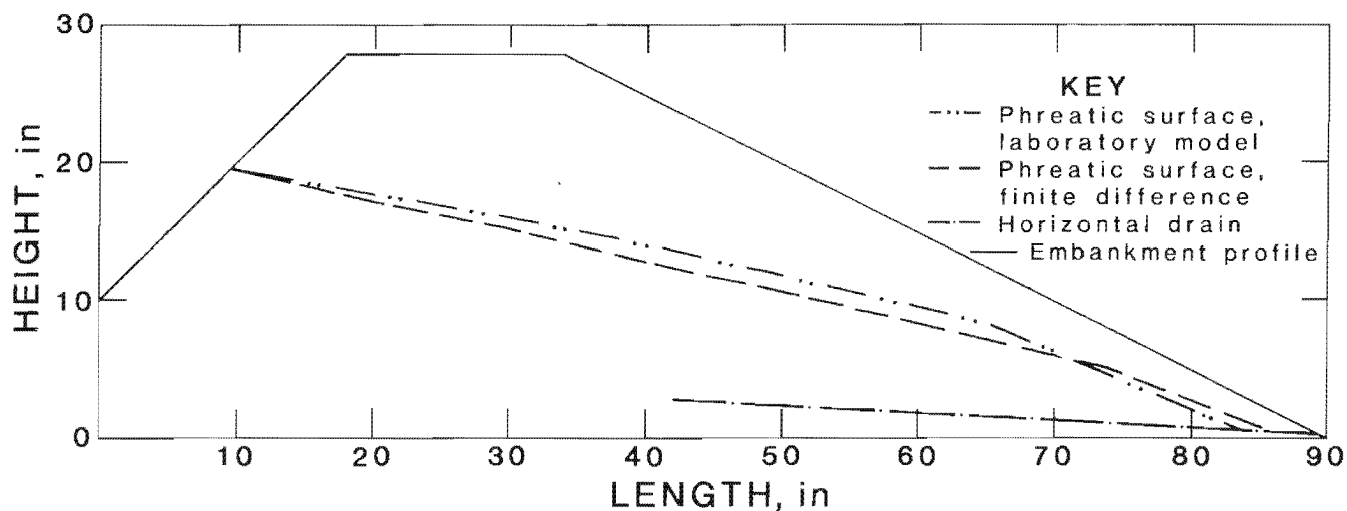


FIGURE 35. — Phreatic surface between drains, laboratory model versus finite-difference method; 48-in drains, 72-in spacing.

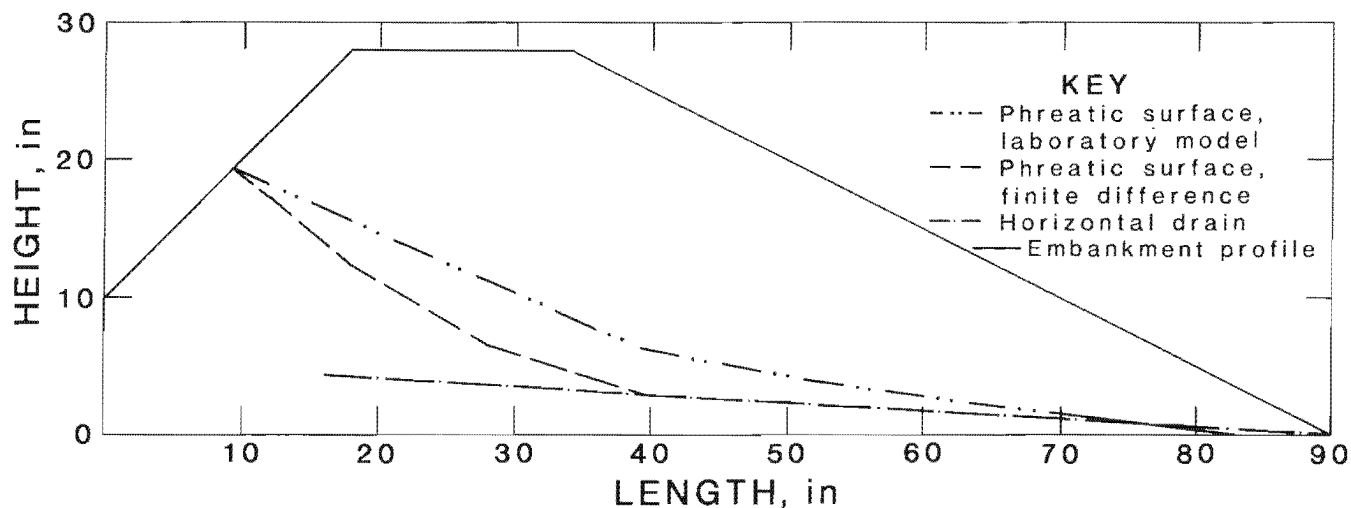


FIGURE 36. — Phreatic surface between drains, laboratory model versus finite-difference method; 72-in drains, 18-in spacing.

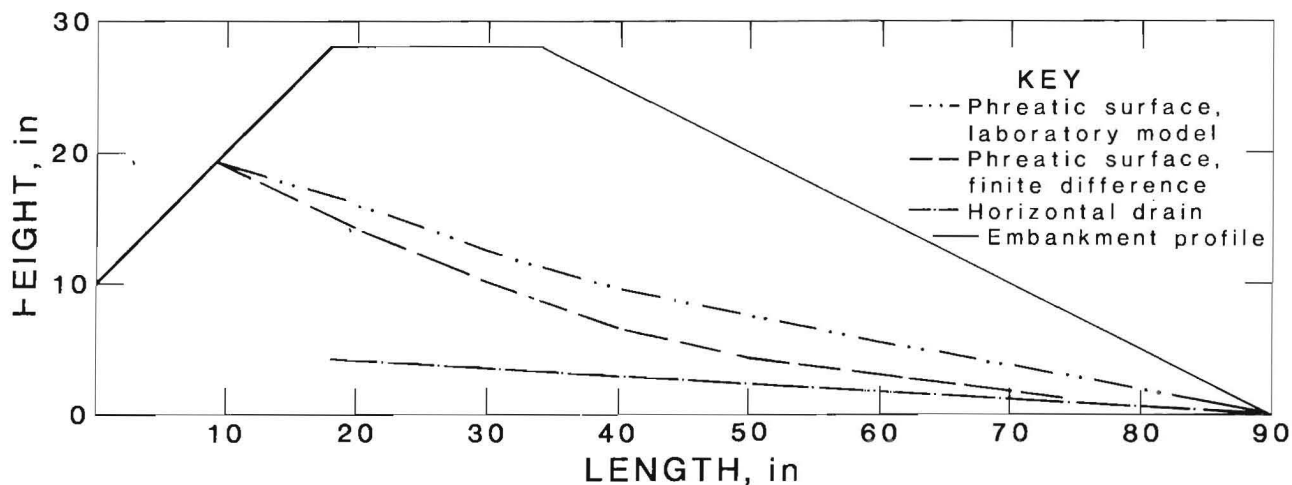


FIGURE 37. — Phreatic surface between drains, laboratory model versus finite-difference method; 72-in drains, 36-in spacing.

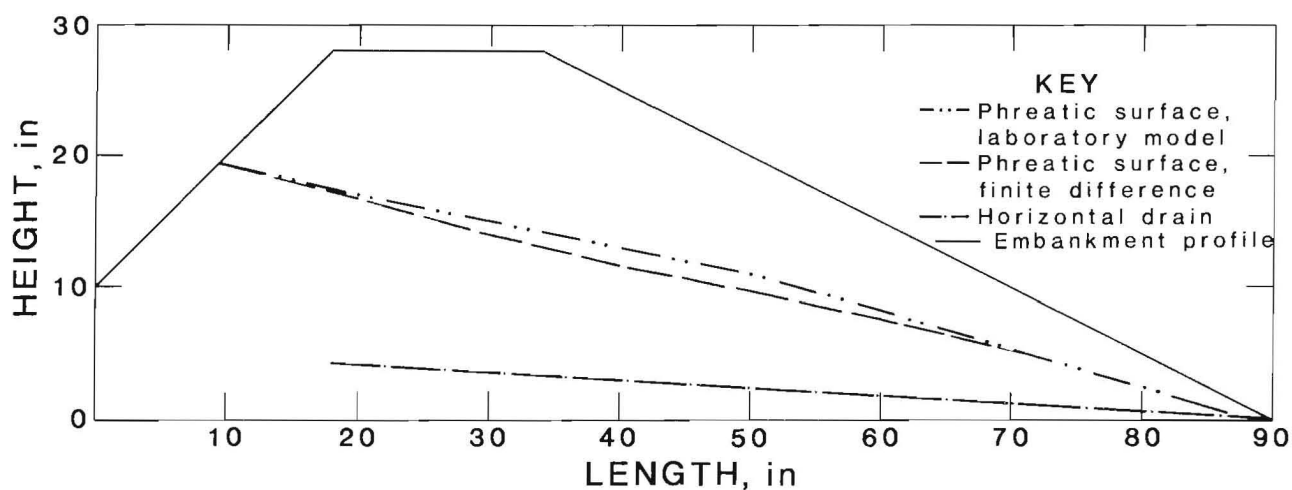


FIGURE 38. — Phreatic surface between drains, laboratory model versus finite-difference method; 72-in drains, 72-in spacing.

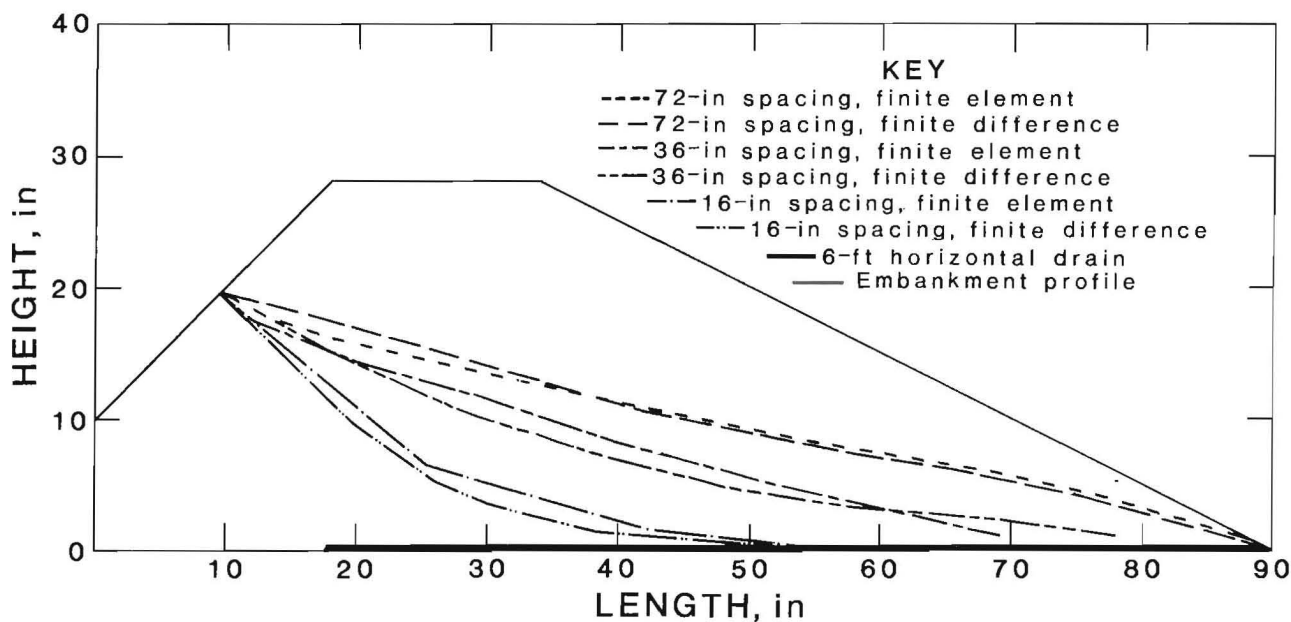


FIGURE 39. — Phreatic surface between drains, finite-element method versus finite-difference method.

## COMPARISON WITH OTHER LABORATORY DATA

Results from the three-dimensional finite-element code are compared to piezometric elevations measured from a seepage-model experiment conducted by Kenney, Pazin, and Choi (7) in figures 40 and 41. The material used to construct the model was glass beads with less than 30 pct retained on the No. 100 sieve, and more than 70 pct was retained on the No. 200 sieve. Drains consisted of 0.2-in drain rods double-wrapped with No. 200 sieve stainless steel mesh, and spot soldered.

Phreatic surfaces calculated by the finite-element code were higher than those measured in the laboratory. For the

case of no horizontal drains (fig. 41), the maximum difference of approximately 0.87 in occurred at a toe-to-piezometer distance of 16 in. When horizontal drains 27 in long and with a spacing of 32 in were installed, the maximum difference was 0.8 in, which occurred at a toe-to-piezometer distance of 32 in.

The results calculated from the computer codes (previously shown to be nearly the same for both codes) were bounded by the measured results from Kenney, Pazin, and Choi's and the Bureau's laboratory models. The phreatic surfaces measured by Kenney, Pazin and Choi were slightly lower than those indicated by the code-generated results, and the phreatic surfaces measured using the Bureau's model were slightly higher.

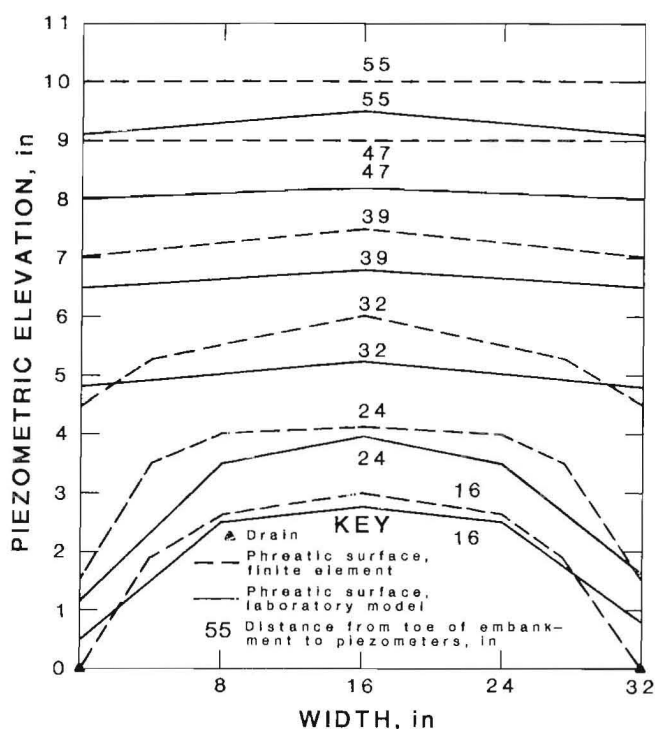


FIGURE 40. — Three-dimensional finite-element results versus piezometric elevations from Kenney, Pazin, and Choi (7); 27-in drains, 32-in spacing.

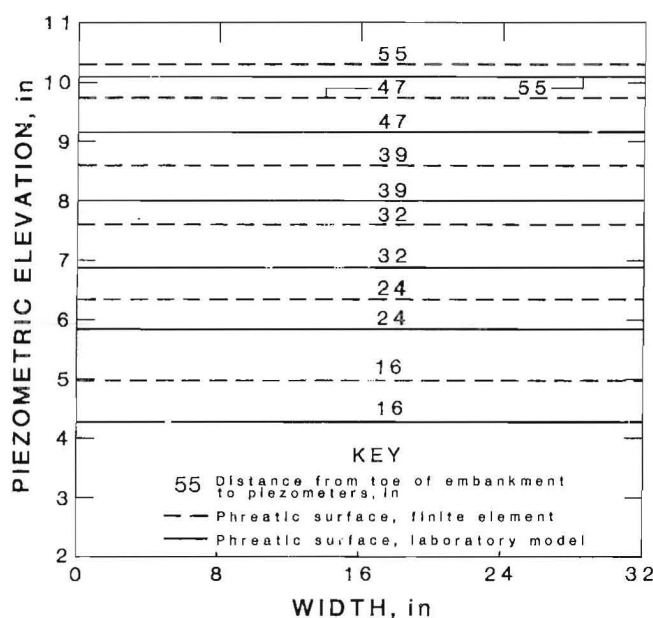


FIGURE 41. — Three-dimensional finite-element results versus piezometric elevations from Kenney, Pazin, and Choi (7); no drains.

## COMPUTER CODES VERSUS FIELD DATA

Piezometric data from two tailings embankments were compared to results calculated using the two-dimensional finite-difference computer code. Although neither embankment had perfectly parallel horizontal drains and piezometer readings between drains were not extensive, each of the embankments provided a basis for comparing the general effects of the drains to the computer model.

In one of the embankments (owned by the Sohio Western Mining Co.), the horizontal drains were installed in array-like patterns with five drains in each array (fig. 42) (8, 15).

The area that was modeled using the finite-difference code is indicated by crosshatching. The boundary conditions and governing equation were as shown in figure 6, with the additional condition that line AB was a no-flow boundary. This boundary condition was used since the face of the starter dam was clogged with fines (15).

A cross-sectional view comparing the computer results to the piezometric data is shown in figure 43. The modeled phreatic surface oscillated about the measured phreatic surface; however, the general trend was the same.

The other embankment studied (owned by Union Carbide Co.) contained filter pads in addition to horizontal drains. This situation was modeled by assigning the nodes representing the filter pads a value of zero. The filter pads were modeled at a 160-ft spacing. The resulting phreatic surface is shown in figure 44. Only readings from one piezometer were available; they ranged from 0 to 2 ft over a period of 8-1/2 yr. The finite-difference method predicted a value of 8 ft.

In summary, the phreatic surface predicted by the finite-difference code was above the measured phreatic surface in one field application and followed the general trend of the phreatic surface in the other. The modeled phreatic surfaces were bounded by the results from the two laboratory experiments.

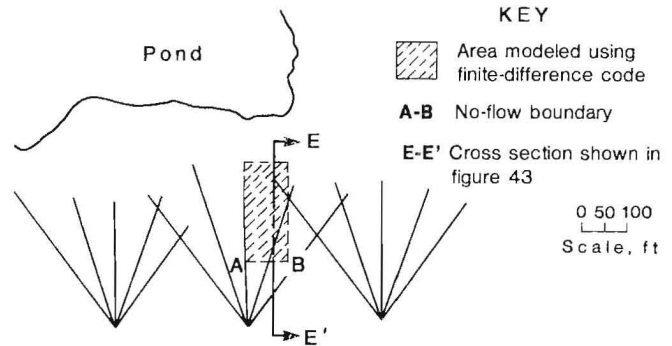


FIGURE 42. — Section of drain arrays showing area modeled using finite-difference code (8).

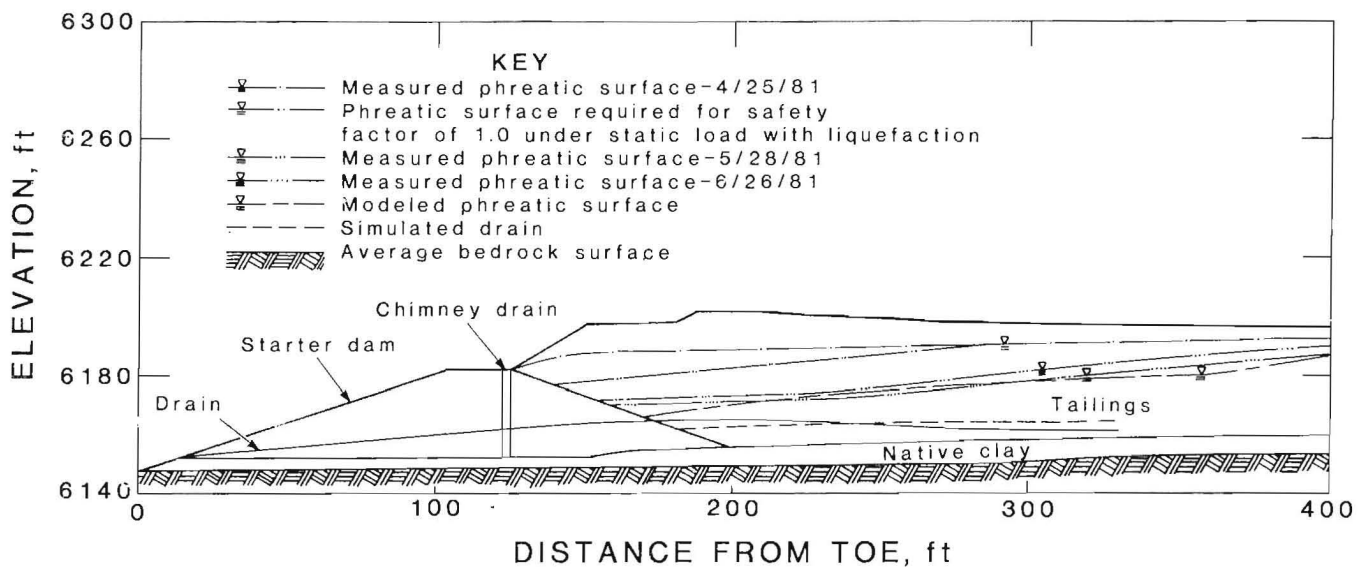


FIGURE 43. — Section E-E' from figure 42, Sohio Western Mining Co. tailings embankment (8).

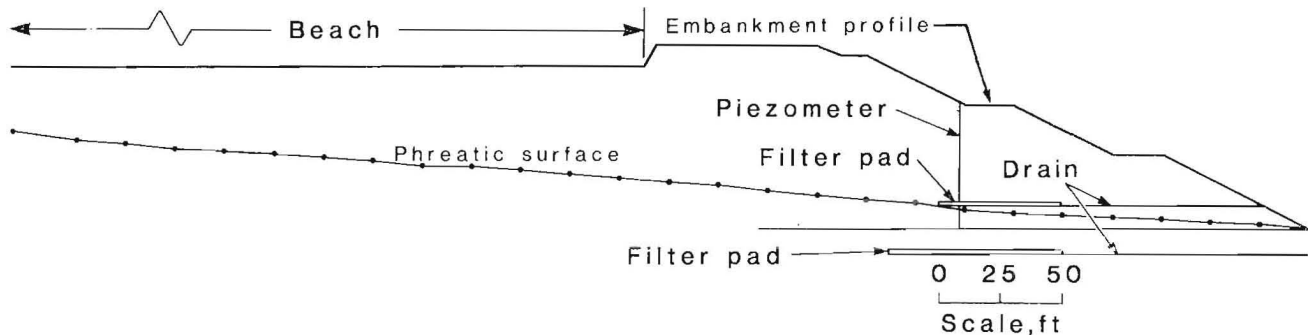


FIGURE 44. — Cross section between filter pads, Union Carbide Corp. tailings embankment.

## DIMENSIONLESS PHREATIC PROFILES

Profiles of phreatic surfaces between drains are presented in figures 45-65 for various drain length and spacing configurations. All parameters are normalized by the distance  $L$ —the distance from the headwater to the toe of the embankment. The ratio  $H/L$  is given for increments of 0.2, 0.25, 0.3,

0.35, 0.4, 0.45, and 0.5, where  $H$  is the vertical distance between the drain and the headwater. The ratio  $l/L$  is given for increments of 0.25, 0.375, and 0.5, where  $l$  is the length of the drain. The curves, representing predicted phreatic surface profiles for various drain spacings ( $S/L$ ) are bounded by

a blanket-drain curve and a "no-drain" curve. (The criterion for increments of  $S/L$  was graph readability.) The following example illustrates how the graphs could be used:

1. Plot the cross section of the embankment. See figure 66 for the cross section used in this example.

2. Determine the distance between the drains and the headwater ( $H$ ) and the horizontal distance from the toe of the embankment to the point at which the pond intersects the upstream slope ( $L$ ). For this example,  $H = 90$  ft and  $L = 250$  ft.

3. Calculate  $H/L$ .  $H/L = 90 \text{ ft}/250 \text{ ft} = 0.36$ .

4. Find the value of  $H/L$  from the graphs that is closest to the value calculated in step 3. For the example, the closest value is 0.35 (figs. 48, 55, and 62).

5. Select the desired drain length ratio  $l/L$ . For illustration, 0.5 is chosen for  $l/L$ , representing a drain length of  $0.5 \times 250 \text{ ft} = 125 \text{ ft}$ . The graph representing  $H/L = 0.35$  (step 4) and  $l/L = 0.5$  is figure 62.

6. Select the phreatic profile desired from the figure. The phreatic surface described by  $S/L = 0.2$  is chosen for this example; this represents a horizontal drain spacing of  $0.2 \times 250 \text{ ft} = 50 \text{ ft}$ .

7. From the  $S/L$  curve selected, read the values of  $h/L$  at several values of  $x/L$ . ( $x$  is the horizontal distance from the pond embankment contact to a point on the horizontal axis, and  $h$  is the water height at distance  $x$ .)

8. Calculate  $(x/L) \times L$  and  $(h/L) \times L$ . Table 1 shows conversions from the dimensionless values to units of the embankment used in the example.

9. Plot the products from step 8 on the cross section of the embankment.

10. Repeat the above process for various drain length and spacing combinations if desired.

As  $L$  becomes larger, it may be desirable to interpolate between graphs to obtain a better estimate of the phreatic surface.

Factor of safety analyses using the Simplified Bishop Method of Slices (2) were performed on the example embankment used in the above example, without drains and with drains spaced 50 ft apart ( $S/L = 0.2$ ). Table 2 shows the conversion from the dimensionless curve values of figure 62 to units of that example embankment for the case of no drains.

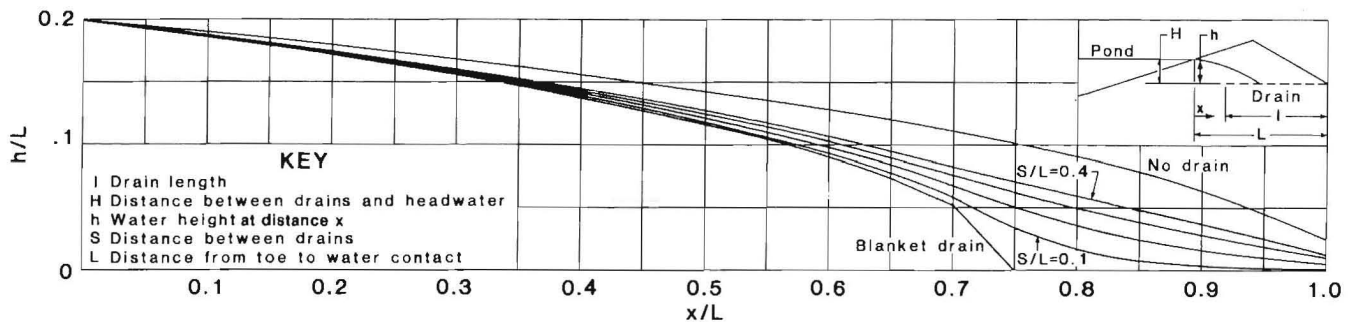


FIGURE 45. — Dimensionless phreatic profiles;  $H/L = 0.2$ ,  $l/L = 0.25$ .

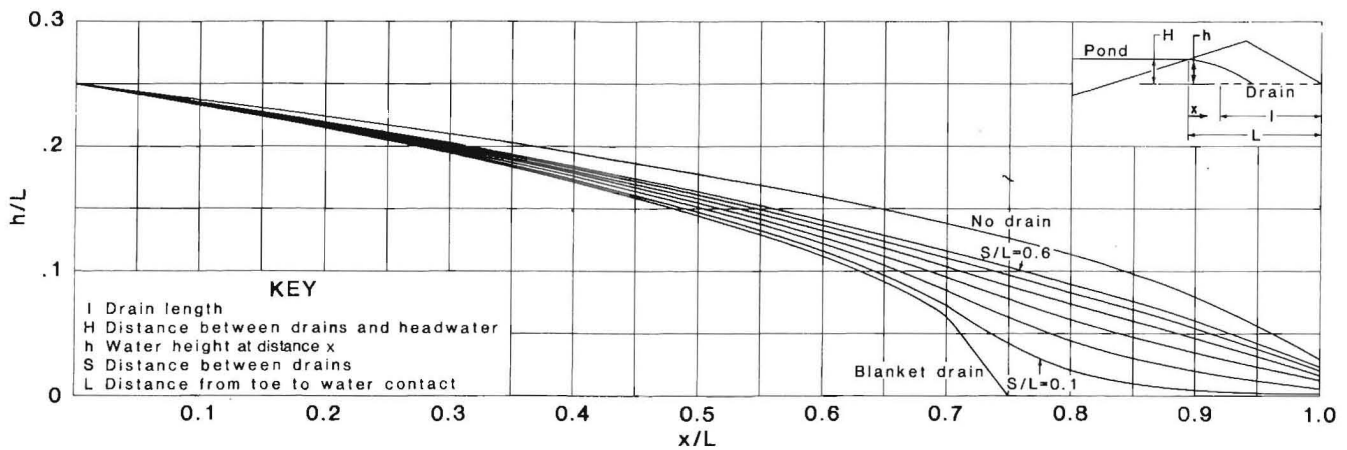
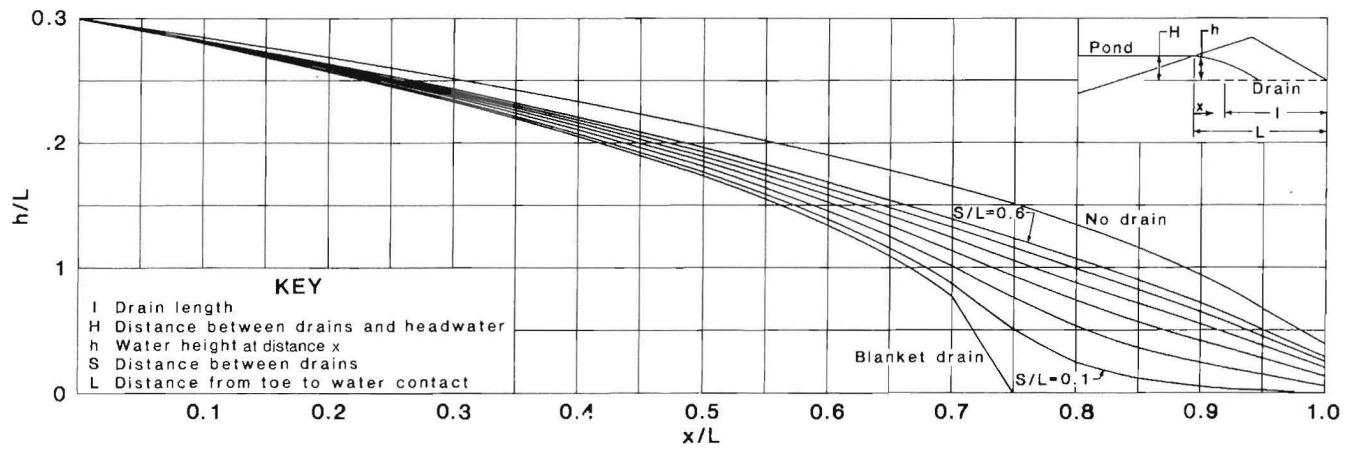
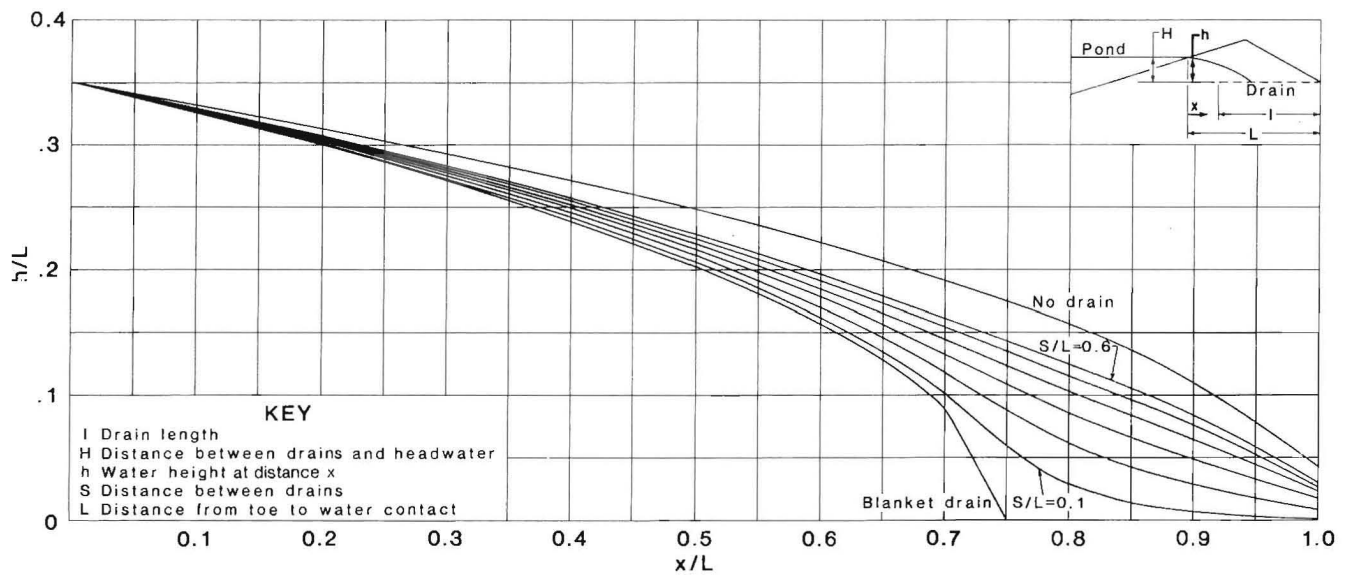
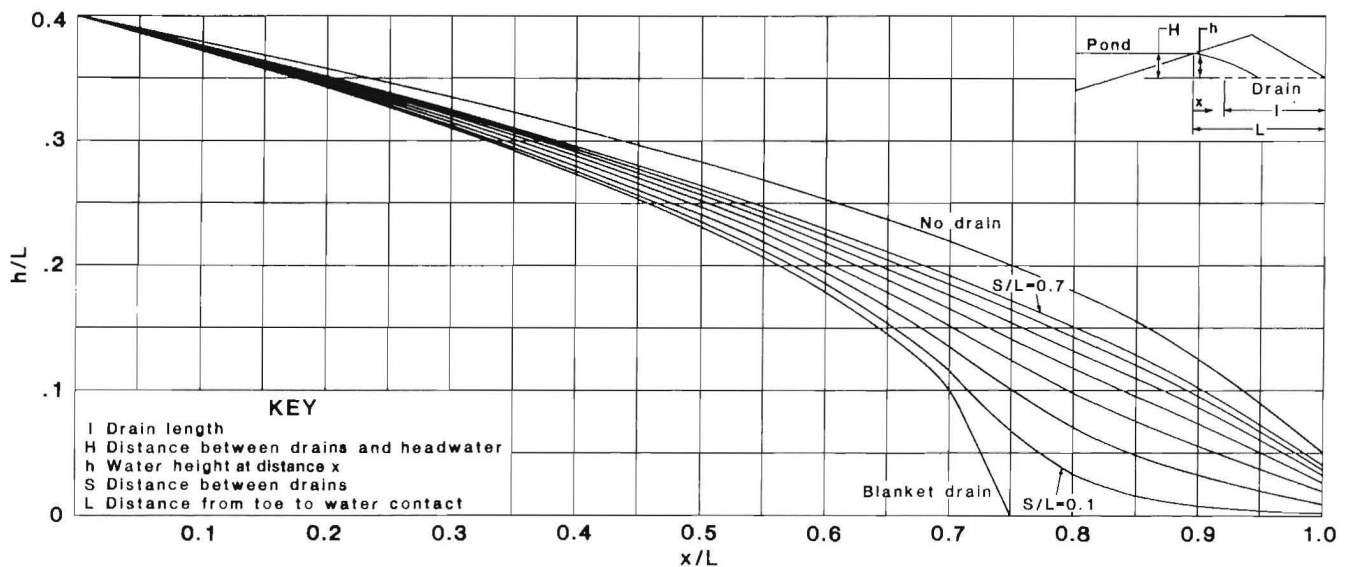


FIGURE 46. — Dimensionless phreatic profiles;  $H/L = 0.25$ ,  $l/L = 0.25$ .

FIGURE 47. — Dimensionless phreatic profiles;  $H/L = 0.3$ ,  $l/L = 0.25$ .FIGURE 48. — Dimensionless phreatic profiles;  $H/L = 0.35$ ,  $l/L = 0.25$ .FIGURE 49. — Dimensionless phreatic profiles;  $H/L = 0.4$ ,  $l/L = 0.25$ .

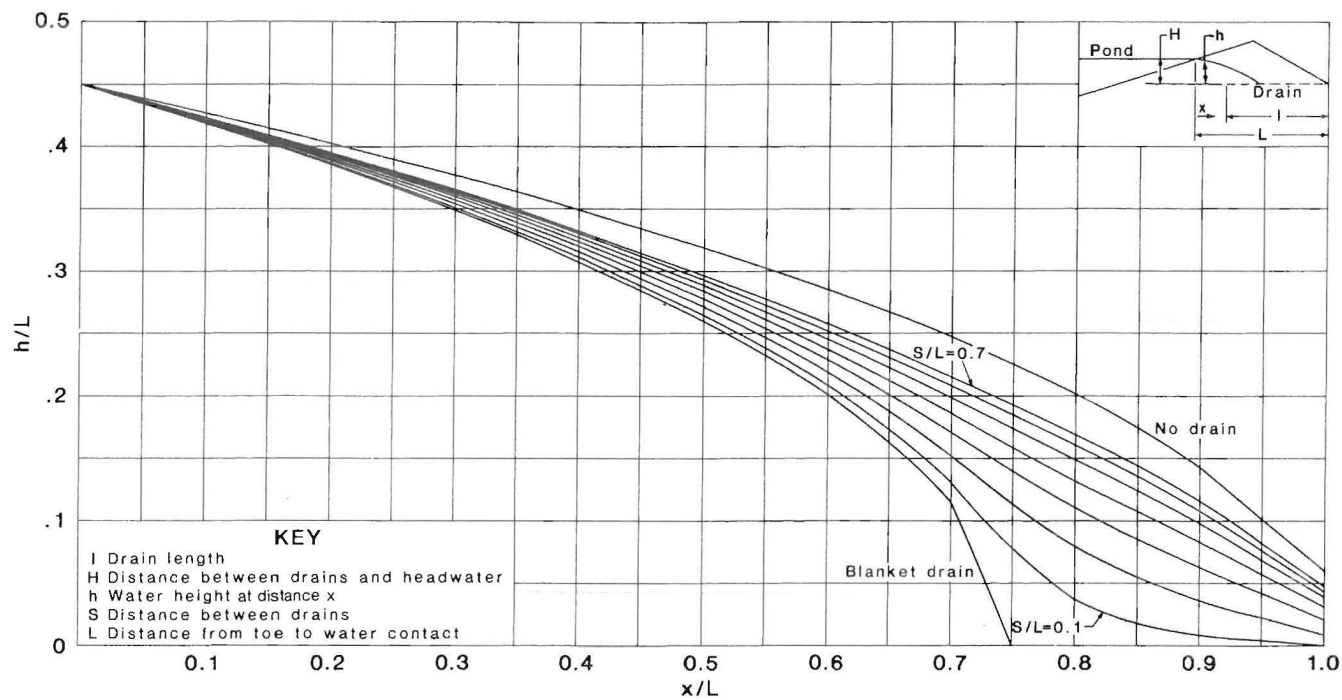


FIGURE 50. — Dimensionless phreatic profiles;  $H/L = 0.45$ ,  $l/L = 0.25$ .

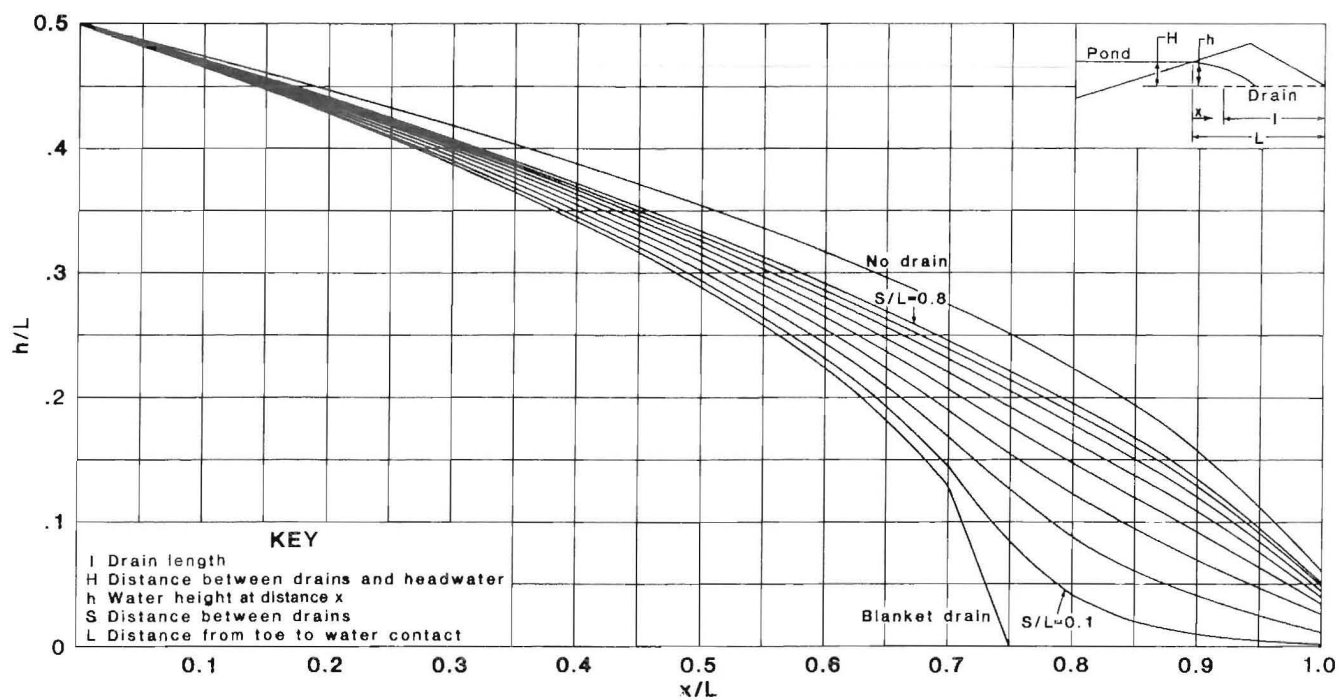
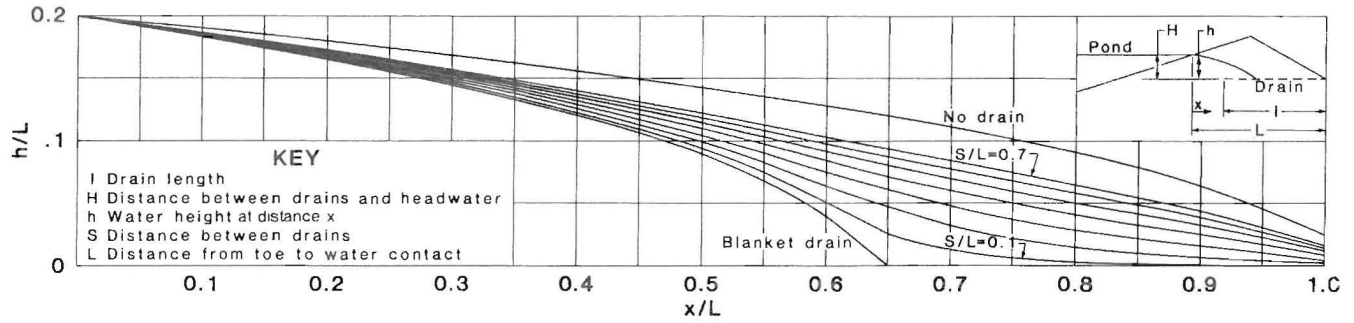
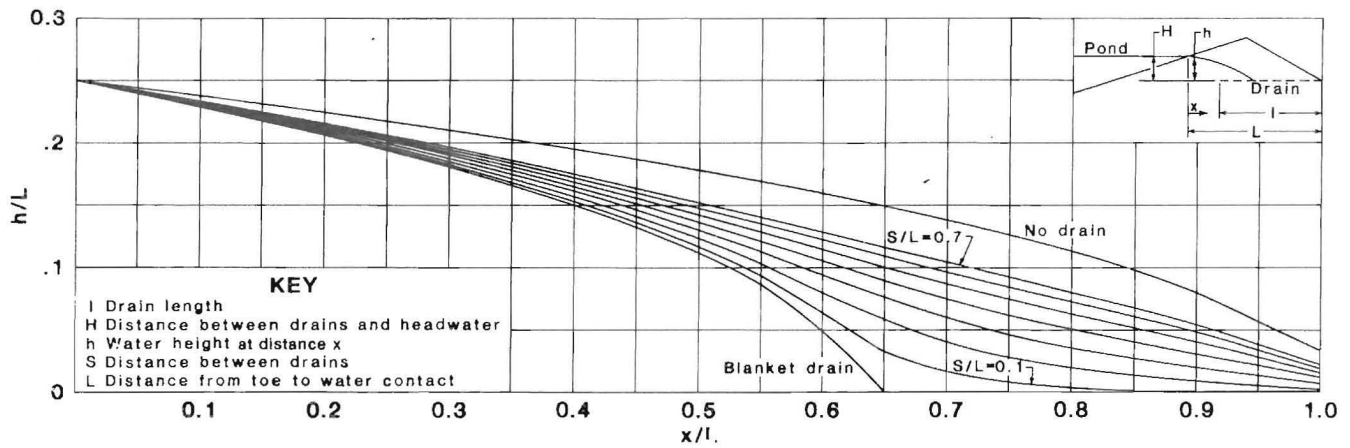
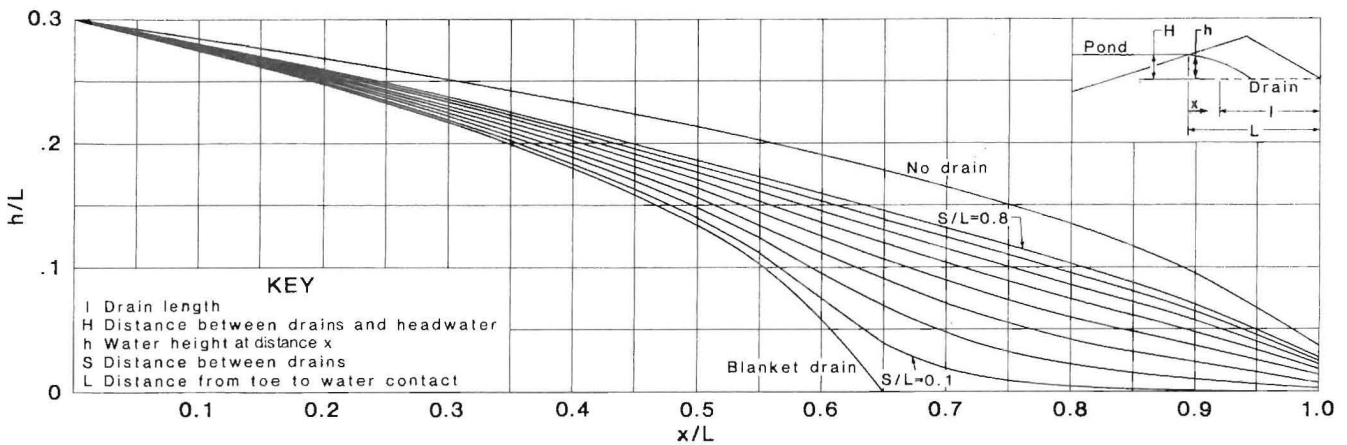
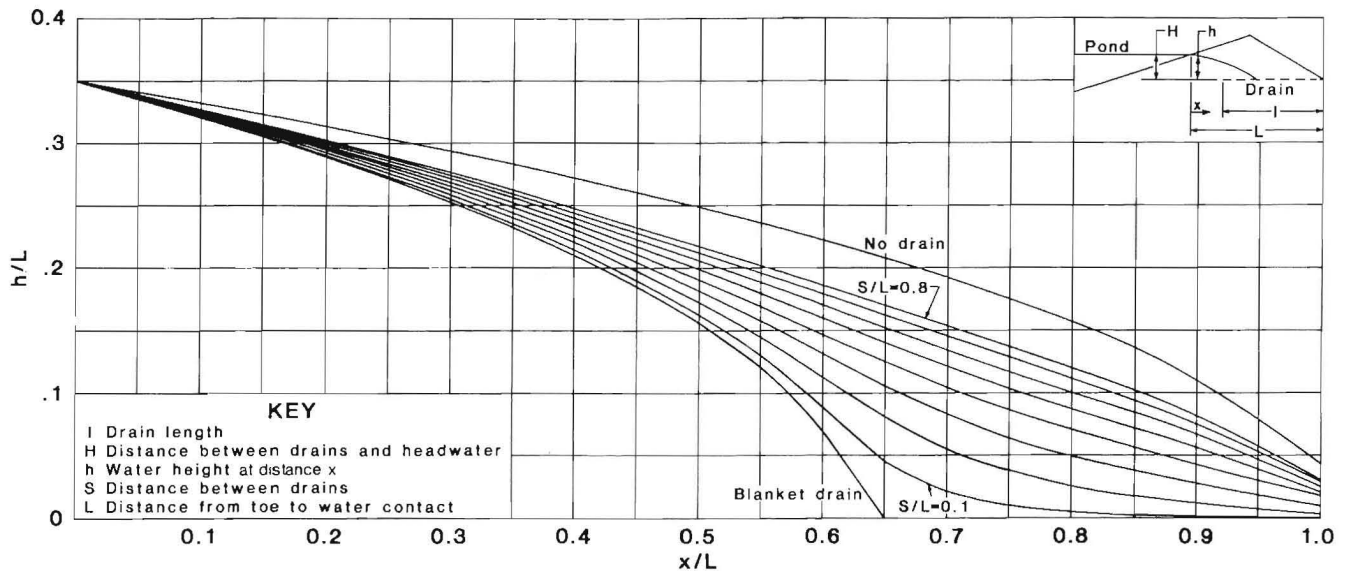
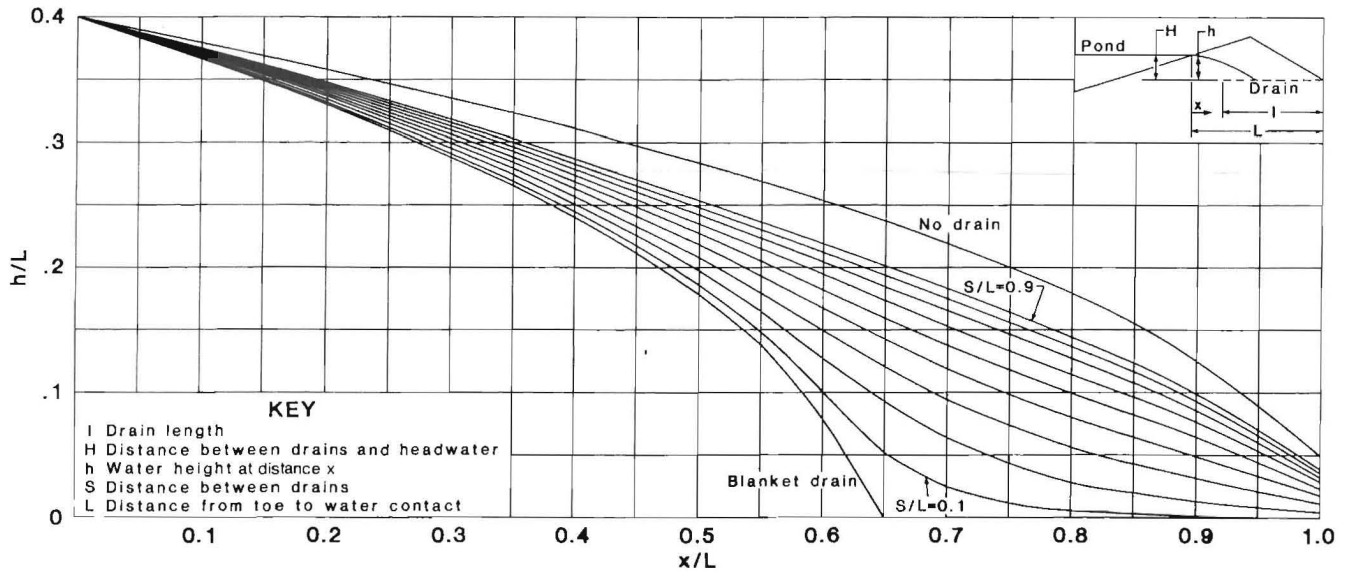


FIGURE 51. — Dimensionless phreatic profiles;  $H/L = 0.5$ ,  $l/L = 0.25$ .

FIGURE 52. — Dimensionless phreatic profiles;  $H/L = 0.2$ ,  $l/L = 0.375$ .FIGURE 53. — Dimensionless phreatic profiles;  $H/L = 0.25$ ,  $l/L = 0.375$ .FIGURE 54. — Dimensionless phreatic profiles;  $H/L = 0.3$ ,  $l/L = 0.375$ .

FIGURE 55. — Dimensionless phreatic profiles;  $H/L = 0.35$ ,  $l/L = 0.375$ .FIGURE 56. — Dimensionless phreatic profiles;  $H/L = 0.4$ ,  $l/L = 0.375$ .

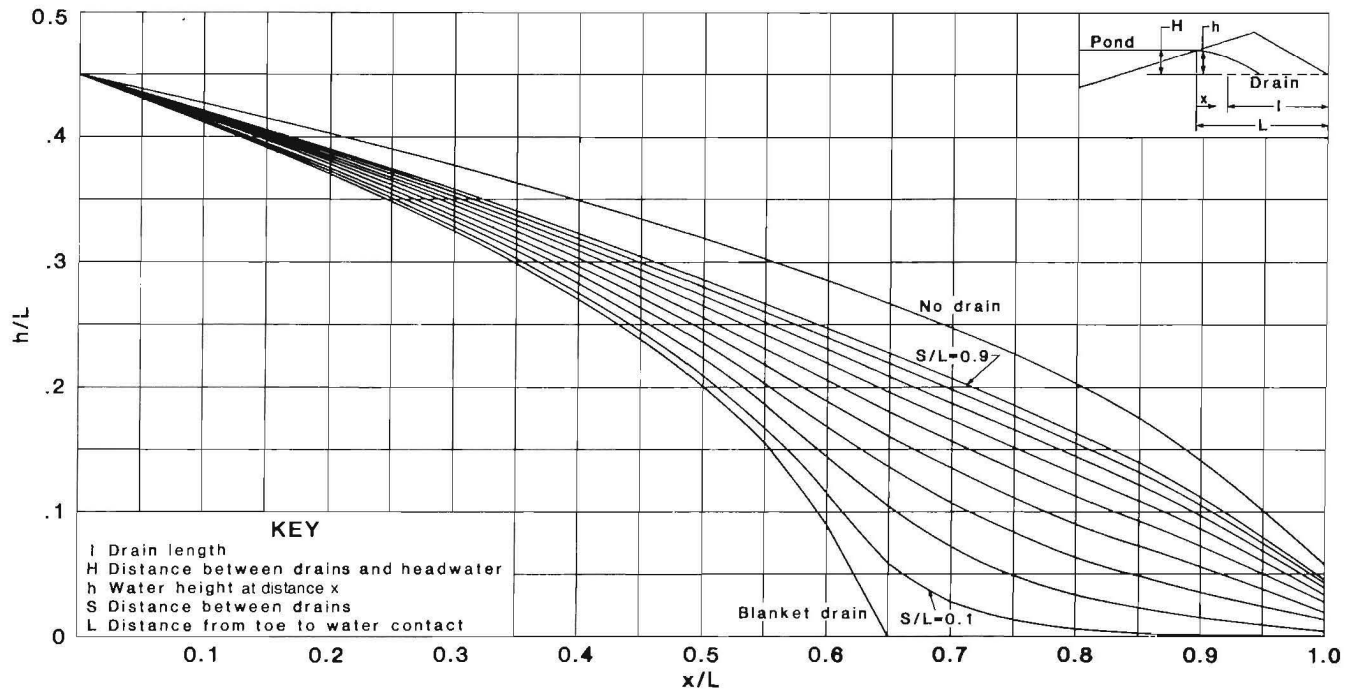


FIGURE 57. — Dimensionless phreatic profiles;  $H/L = 0.45$ ,  $l/L = 0.375$ .

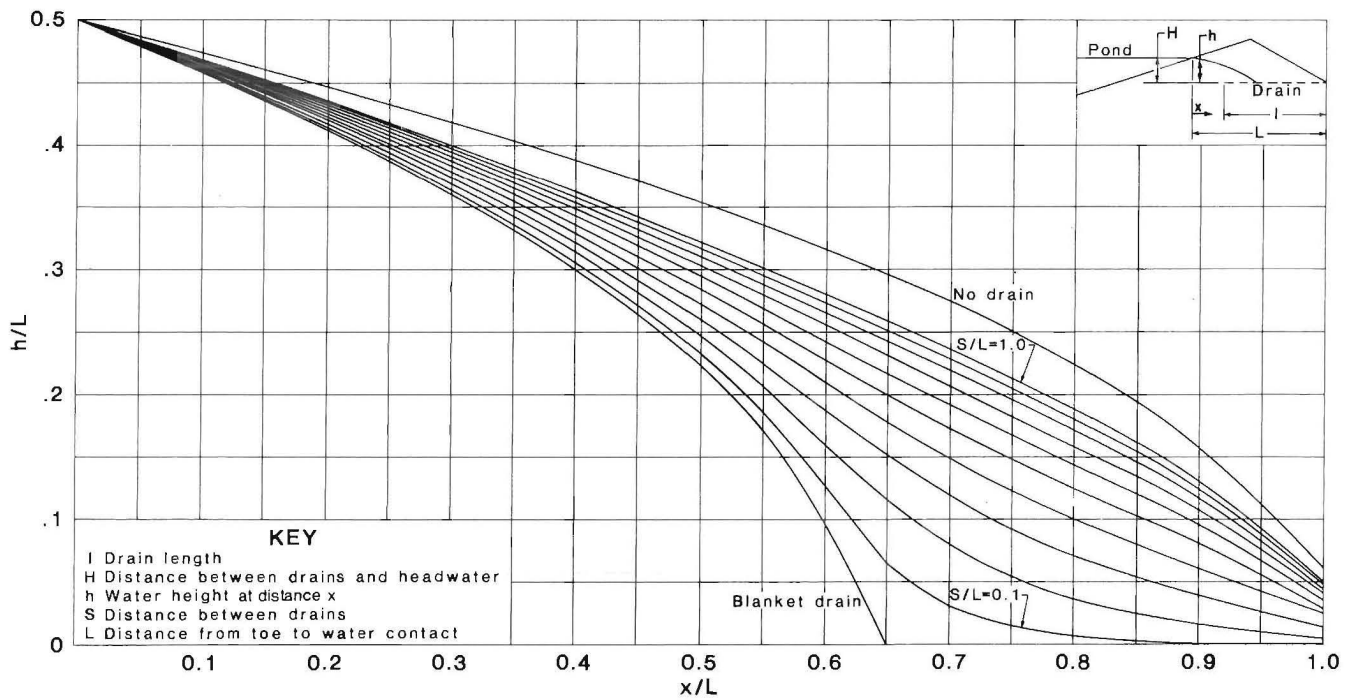
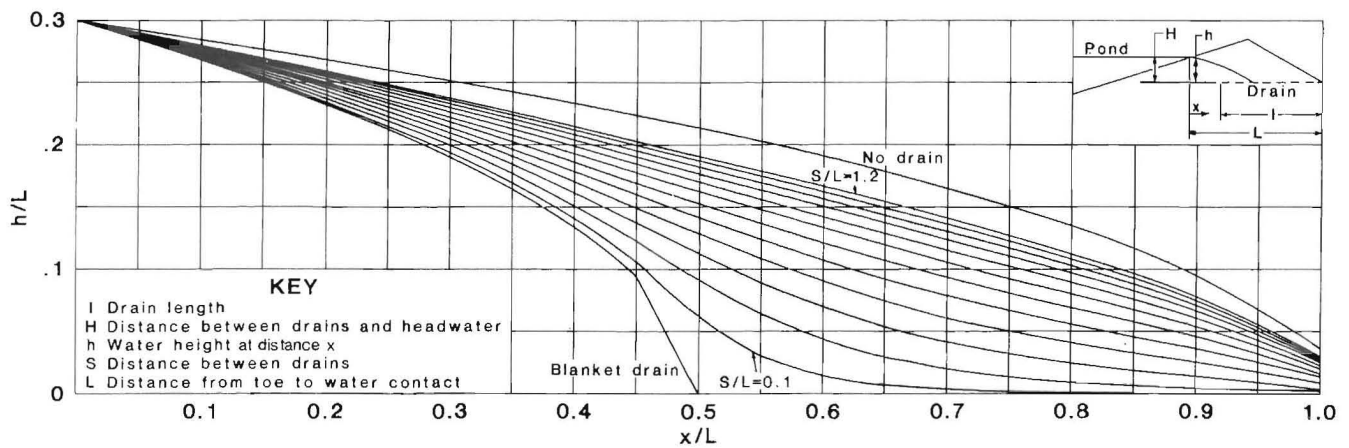
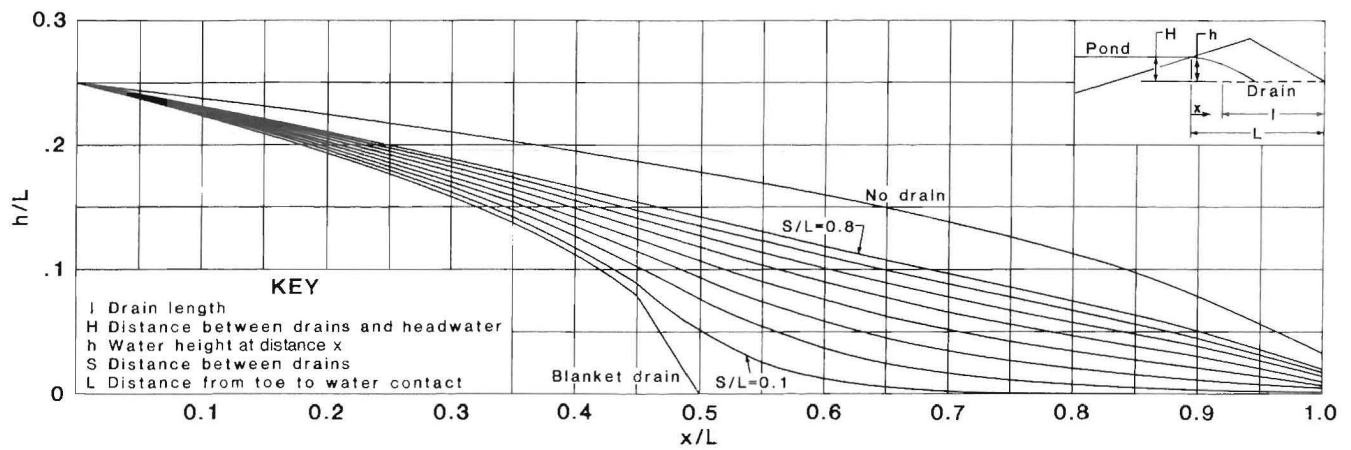
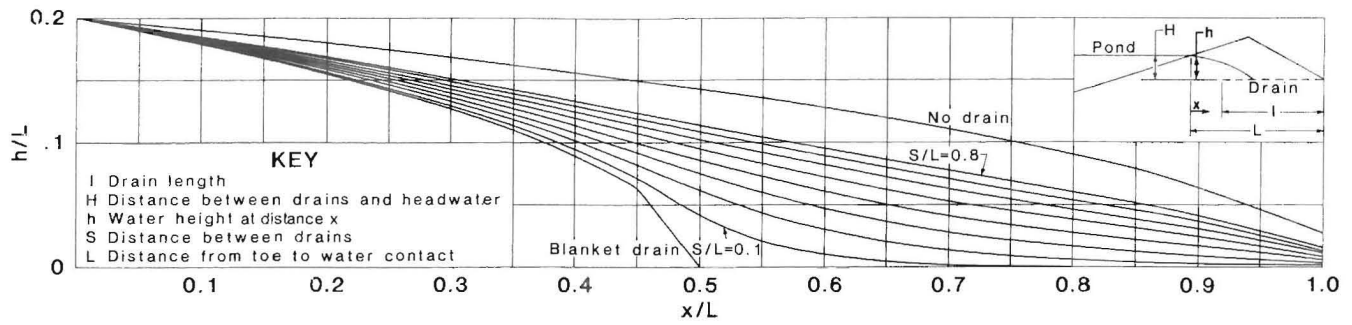


FIGURE 58. — Dimensionless phreatic profiles;  $H/L = 0.5$ ,  $l/L = 0.375$ .



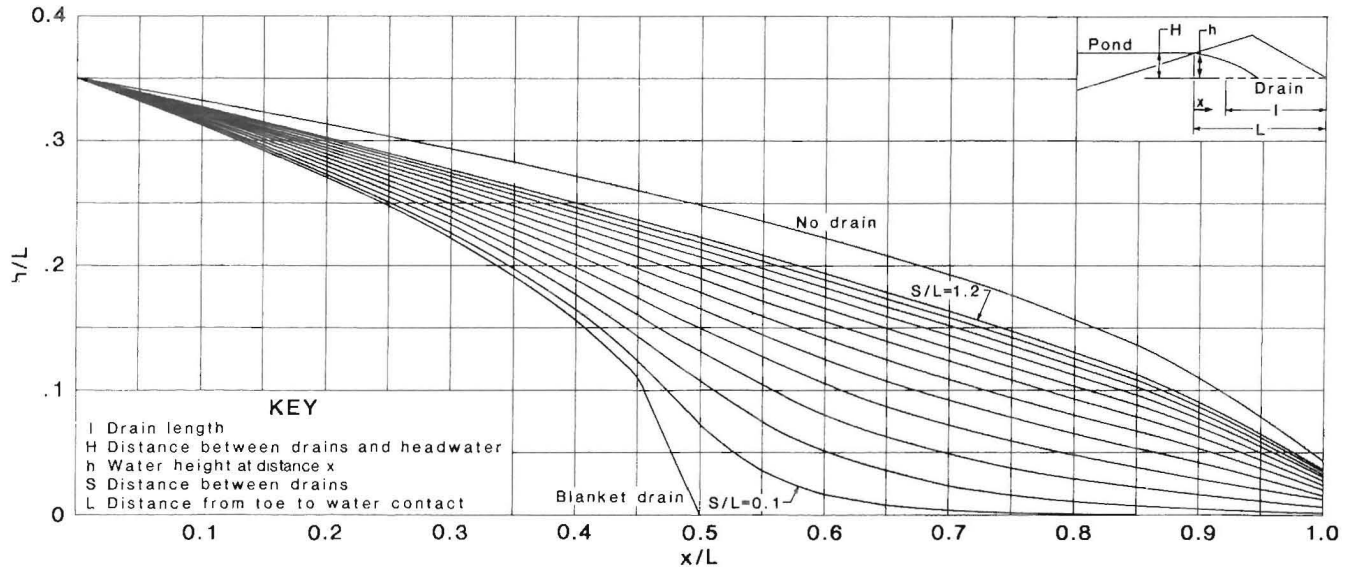


FIGURE 62. — Dimensionless phreatic profiles;  $H/L = 0.35$ ,  $l/L = 0.5$ .

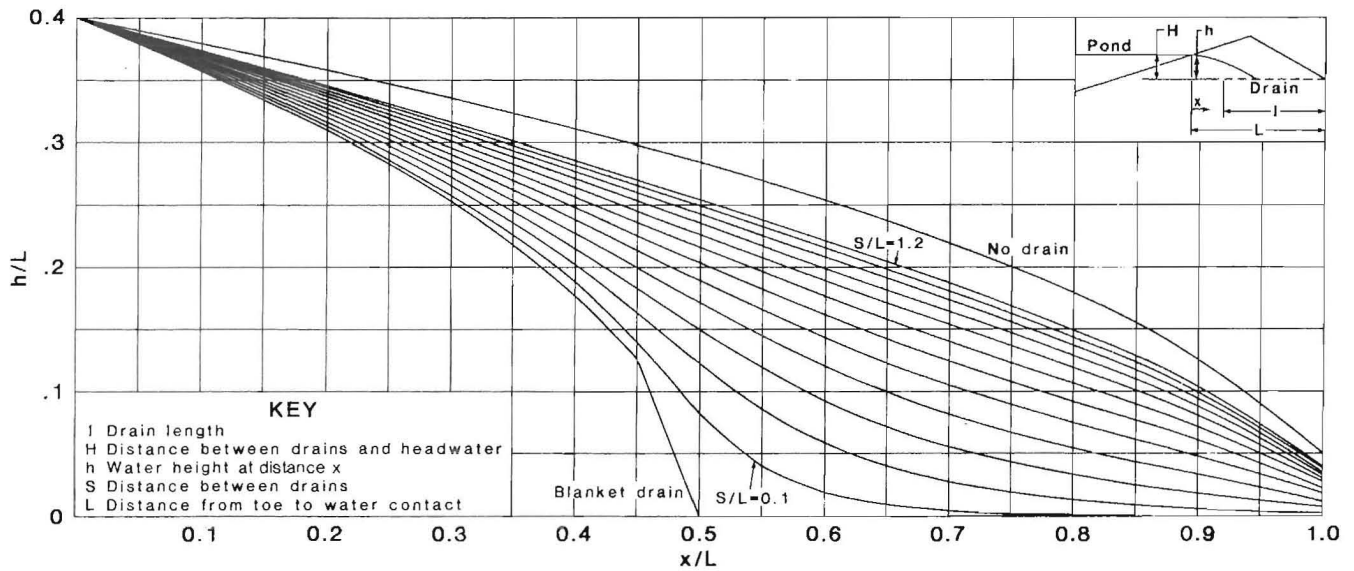


FIGURE 63. — Dimensionless phreatic profiles;  $H/L = 0.4$ ,  $l/L = 0.5$ .

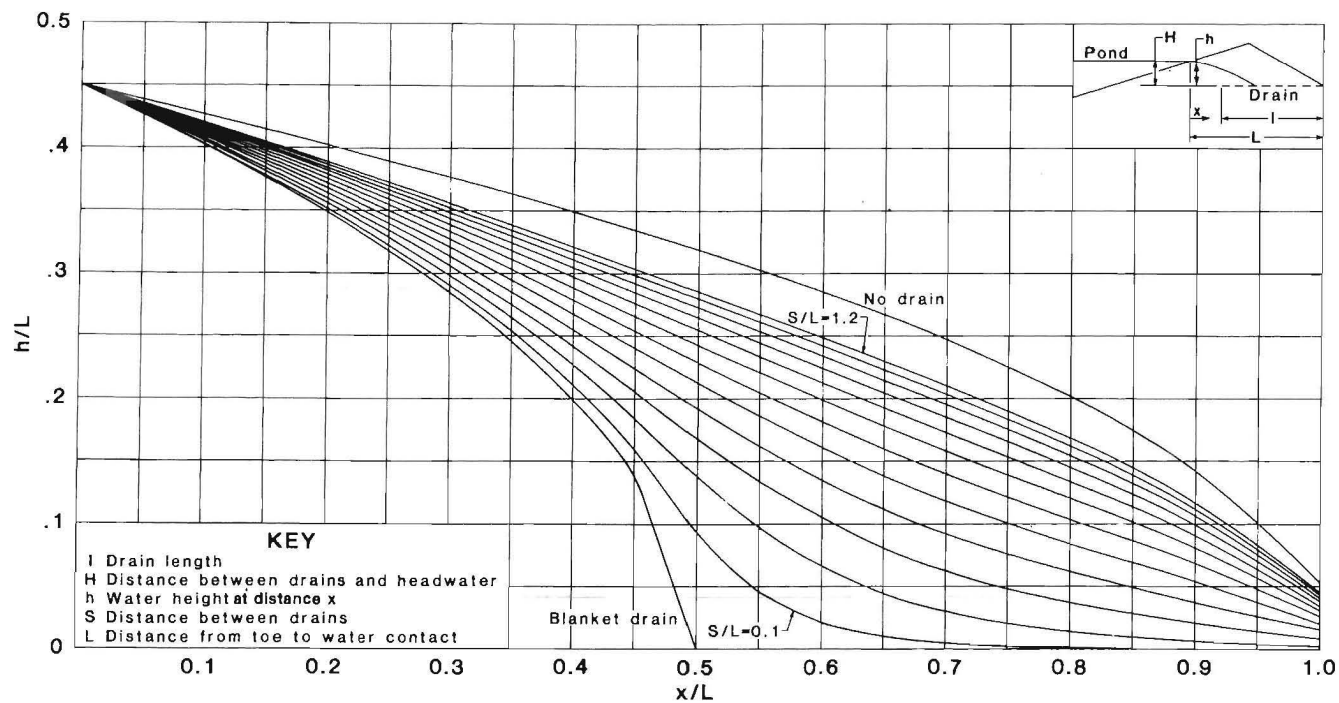
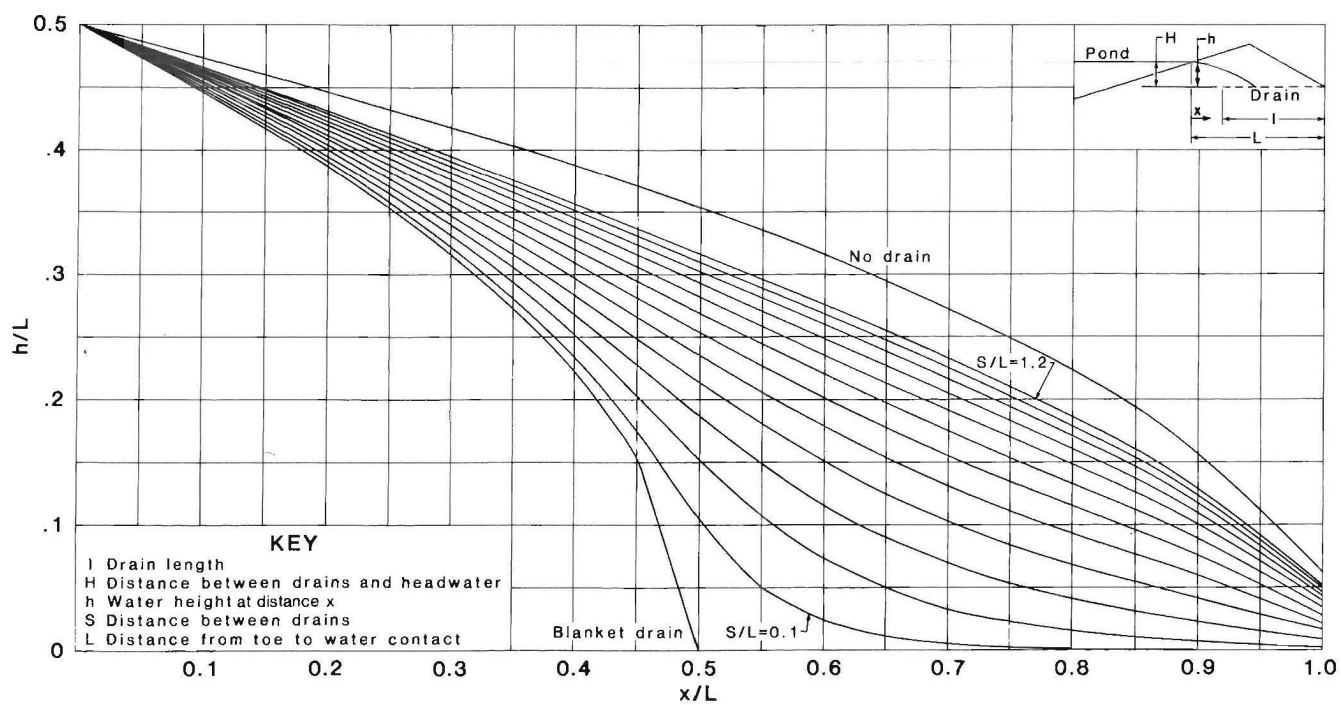
FIGURE 64. — Dimensionless phreatic profiles;  $H/L = 0.45$ ,  $l/L = 0.5$ .FIGURE 65. — Dimensionless phreatic profiles;  $H/L = 0.5$ ,  $l/L = 0.5$ .

TABLE 1. - Conversion from dimensionless graph values to units used in example, drains 50 ft apart

( $H = 90$  ft,  $L = 250$  ft,  $S/L = 0.2$ ,  
 $l/L = 0.5$ , and  $H/L = 0.35$ .)

Point <sup>1</sup>	Dimensionless tables		Values calculated for example	
	$x/L$	$h/L$	$\frac{x}{L} \cdot L$ , ft	$\frac{h}{L} \cdot L$ , ft
1	0.0	0.35	0.0	87.5
2	.1	.32	25.0	80.0
3	.2	.28	50.0	70.0
4	.3	.23	75.0	57.5
5	.4	.18	100.0	45.0
6	.5	.11	125.0	27.5
7	.6	.05	150.0	12.5
8	.7	.03	175.0	7.5
9	.8	.01	200.0	2.5
10	.9	.001	225.0	.3

<sup>1</sup>Points identified in figure 66.

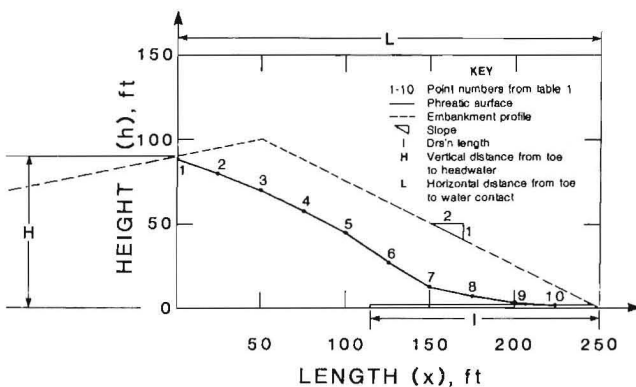


FIGURE 66. — Embankment cross section plotted using dimensionless graphs.

The soil lying beneath the phreatic surface was assumed to be fully saturated and to have the following physical properties:

Angle of internal friction .....  $30^\circ$   
Cohesion ..... 10 psi  
Density ..... 110 pcf

TABLE 2. - Conversion from dimensionless graph values to units used in example, no-drains case

( $H = 90$  ft,  $L = 250$  ft, and  $H/L = 0.35$ .)

Point <sup>1</sup>	Dimensionless tables		Values calculated for example	
	$x/L$	$h/L$	$\frac{x}{L} \cdot L$ , ft	$\frac{h}{L} \cdot L$ , ft
1	0.0	0.35	0.0	87.5
2	.1	.34	25.0	85.0
3	.2	.32	50.0	80.0
4	.3	.29	75.0	72.5
5	.4	.28	100.0	70.0
6	.5	.25	125.0	62.5

<sup>1</sup>Points identified in figure 67.

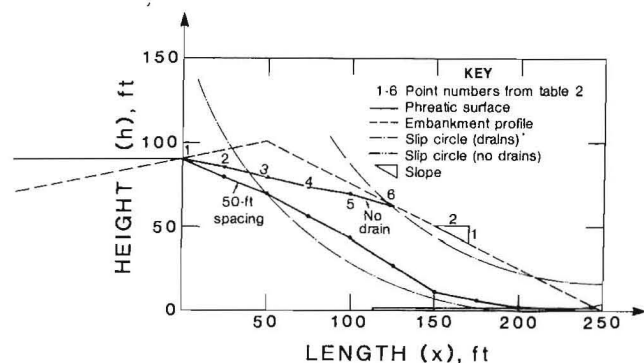


FIGURE 67. — Slip circles for embankment plotted in figure 66.

The soil above the phreatic surface was assumed to have no capillary zone and to have the following physical properties:

Angle of internal friction .....  $35^\circ$   
Cohesion ..... 10 psi  
Density ..... 95 pcf

Figure 67 shows the phreatic surfaces for the two cases, along with the respective slip circles. The embankment used as an example illustrates the importance of a low phreatic surface, since the factor of safety is increased from 0.51 for the case of no drains to 1.3 for the case of drains spaced 50 ft apart (fig. 67).

## CONCLUSIONS AND LIMITATIONS

The two-dimensional finite-difference and three-dimensional finite-element computer codes produced nearly the same results for phreatic surface locations between horizontal drains.

The phreatic surfaces predicted using the above codes were between the phreatic surfaces of two laboratory models and slightly above the phreatic surface of one field application. The phreatic surface from the second field application

matched the code-generated phreatic surface closely. Differences between the code-generated phreatic surfaces and those measured in the models and in the field can be attributed to some combination of the following:

1. Piezometric measurement error (clogged filters, measurement accuracy, etc.).
2. The assumption in the computer models that permeability is not a function of location in the embankment.

3. Variations in upstream pond elevations in the laboratory models and field applications.

Coupled with slope stability analysis, the dimensionless graphs presented herein can provide an estimate of horizontal drain length and spacing dimensions necessary to achieve slope stability.

Nonhomogeneous embankments may require further analysis to determine drain placement

## REFERENCES

1. Abrao, P. C. Open Pit Mine Slopes Drainage Through Horizontal Boreholes. Paper in Water in Mining and Underground Works (Grenada, Spain, Sept. 18-22, 1978). National Association of Mining Engineers, v. 1, 1978, pp. 573-583.
2. Bailey, W. A. Stability Analysis by Limited Equilibrium. C.E. Thesis, MIT, Cambridge, MA, 1966, 153 pp.
3. Casagrande, A. Seepage Through Dams. Trans. N. Eng. Water Works Assoc., v. 51, June 1937, pp. 296-336.
4. Corp, E. L., R. L. Schuster, and M. M. McDonald. Elastic-Plastic Stability Analysis of Mine-Waste Embankments. BuMines RI 8069, 1975, 98 pp.
5. Harr, M. E. Groundwater and Seepage. McGraw-Hill, 1962, 315 pp.
6. Kealy, C. D., and R. A. Busch. Determining Seepage Characteristics of Mill-Tailings Dams by the Finite-Element Method. BuMines RI 7477, 1971, 113 pp.
7. Kenney, T. C., M. Pazin, and W. S. Choi. Design of Horizontal Drains for Soil Slopes. J. Geotech. Eng. Div., Am. Soc. Civ. Eng., v. 103, Nov. 1977, pp. 1311-1323.
8. Kuhn, A. K., J. G. Franzone, and J. J. Oliver. Stability Enhancement of Tailings by Horizontal Drainage. Paper in Fifth Annual Uranium Seminar (Albuquerque, NM, Sept. 20-23, 1981). AIME, New York, 1982, 6 pp.
9. Murray, W. A., and P. L. Monkmeyer. Validity of Dupuit-Forchheimer Equation. J. Hydraul. Div., Am. Soc. Civ. Eng., v. 91, Sept. 1973, pp. 1573-1583.
10. Tesarik, D. R., and P. C. McWilliams. Factor of Safety Charts for Estimating the Stability of Saturated and Unsaturated Tailings Pond Embankments. BuMines RI 8564, 1981, 97 pp.
11. Tracy, F. T. A Plane and Axisymmetric Finite Element Program for Steady-State and Transient Seepage Problems. U.S. Army Eng. Waterways Exp. Sta., Vicksburg, MS, Misc. Paper K-73-4, May 1973, 108 pp.
12. \_\_\_\_\_. A Three-Dimensional Finite Element Program for Steady-State and Transient Seepage Problems, U.S. Army Eng. Waterways Exp. Sta., Vicksburg, MS, Misc. Paper K-73-3, May 1973, 220 pp.
13. Verma, R. D., and W. Brutsaert. Unsteady Free Surface Ground Water Seepage. J. Hydraulics Div., Am. Soc. Civ. Eng., v. 97, Aug. 1971, pp. 1213-1229.
14. Wang, H. F., and M. P. Anderson. Introduction to Groundwater Modeling. W. H. Freeman, 1982, 237 pp.
15. Williams, R., G. Bloomsburg, and G. Winter. Inflow to Horizontal Drains in Tailings Embankments (contract J0100013, Williams, Robinette, and Associates). BuMines OFR 26(2)-83, 1982, 49 pp.; NTIS PB 83-178749.